Curvature–Memory Coupling as a Phenomenological Extension of Classical Gravity with Testable Interferometric Signatures

Chaim Zeitz

Affiliation: HDIF Nexus Research Labs

Website: https://chaimz2020.wixsite.com/hdif-nexus

Independent Researcher, Tamarac, United States

Corresponding author: ZeitzChaim@gmail.com

ORCID: 0009-0000-7129-0349

Preprint DOI: 10.5281/zenodo.18644816

March 2026

Abstract

We present a covariant curvature–memory response framework within an effective field theory description of classical gravity, in which the geometric response of spacetime depends causally on prior curvature configurations. In the linearized matter-coupled regime this produces a frequency-dependent phase lag in the scalar curvature response, generating a measurable phase-lag signal in precision atom-interferometer measurements of gravitational acceleration. The modification is implemented variationally by augmenting the Einstein–Hilbert functional with admissible Volterra-type memory terms constructed to preserve diffeomorphism invariance, energy–momentum conservation, causal structure, and stability. In the vanishing-memory limit the theory reduces exactly to Einstein's equations, ensuring consistency with established gravitational tests. No additional propagating tensor degrees of freedom or modifications to vacuum gravitational-wave propagation are introduced. Deviations from general relativity are parameterized by a small phenomenological coupling and a relaxation timescale controlling the retarded response. We derive the explicit mapping from curvature perturbations to interferometric phase and show that the memory response generates a measurable phase lag in precision atom interferometers. A worked near-field benchmark and representative exclusion curves in the $(\alpha_{\text{eff}}, \tau)$ parameter space are presented for experimentally accessible phase sensitivities. The framework is therefore formulated as a minimal phenomenological extension with a well-defined experimentally testable sector designed to constrain possible history-dependent curvature response in matter-coupled gravitational dynamics.

Keywords: General relativity; Modified gravity; Nonlocal gravity; Memory kernels; Atom interferometry

1 Introduction

General relativity (GR) provides a geometric description of gravitation in which spacetime curvature responds locally and instantaneously to stress–energy through Einstein's field equations [1]. Within all experimentally tested regimes, this local constitutive relation between curvature and matter has proven extraordinarily successful.

Nevertheless, from the perspective of effective field theory (EFT) [2], strictly instantaneous response is not generically guaranteed once short-distance or high-frequency structure is coarse-grained. In many classical and quantum systems, effective descriptions admit retarded, nonlocal-in-time corrections while preserving covariance and conservation laws at the macroscopic level. Such history-dependent response is well established in constitutive physics, linear response theory, and effective descriptions of open systems [3, 4, 5, 6].

Importantly, retarded response effects already arise in established effective descriptions of classical gravity. In post-Newtonian gravitational effective field theory, so-called hereditary or "tail" terms encode the influence of prior curvature configurations on present dynamics through explicitly time-nonlocal integrals. Such effects demonstrate that causal history dependence is not incompatible with the geometric structure of GR once additional degrees of freedom or radiation sectors are integrated out. This observation motivates exploring whether a similar, but experimentally accessible, response structure could appear in matter-coupled curvature dynamics at laboratory scales.

A related source of nonlocal gravitational dynamics arises in stochastic semiclassical gravity, where the metric is treated as an open system interacting with quantum matter fields. In that framework, integrating out quantum fluctuations of the matter sector produces effective Einstein–Langevin equations containing retarded dissipation kernels and stochastic noise terms acting on geometric variables [7, 8, 9]. These kernels encode history-dependent response of spacetime geometry arising from coarse-grained microscopic degrees of freedom. While the present work does not derive its curvature–memory kernel from a specific microscopic model, such results demonstrate that causal nonlocal response structures can arise naturally in effective descriptions of gravitational dynamics when additional degrees of freedom are integrated out.

Within an effective-field-theory framework, symmetry and covariance permit additional curvature-response operators beyond the local Einstein–Hilbert term. The present work focuses on a specific class of such operators corresponding to causal Volterra-type memory functionals of curvature invariants. The purpose of this construction is not to assert a particular microscopic origin for these terms, but rather to parameterize a possible class of history-dependent gravitational responses and to develop the observable consequences that would allow them to be experimentally constrained.

The present work adopts this perspective by asking a focused question: can the geometric response sector of classical gravity admit a small, controlled, causal non-Markovian correction consistent with diffeomorphism invariance and exact recovery of GR in its tested domain?

Importantly, the question is not whether GR fails, nor whether vacuum gravitational-wave propagation is modified. Rather, we investigate whether strictly instantaneous curvature response represents an idealization that may admit experimentally testable refinement in matter-coupled regimes.

We explore this possibility by introducing a covariant, kernel-regulated curvature–memory extension of classical gravity. The modification is formulated as a retarded Volterra-type functional confined strictly to the past light cone. No additional propagating tensor degrees of freedom or new matter fields are introduced, and the vacuum graviton sector remains unchanged.

The framework is constructed variationally by augmenting the Einstein–Hilbert action with admissible causal memory terms. The resulting modified field equations reduce exactly to Einstein's equations in the vanishing-memory limit. Deviations are parameterized by a small phenomenological coupling and a relaxation timescale controlling the retarded response. Unlike many nonlocal or modified-gravity frameworks, which typically focus on modified field equations or cosmological phenomenology, the present construction develops the full observable mapping from the curvature-memory kernel to measurable signals.

In the linearized, matter-coupled regime, the theory predicts a frequency-dependent phase lag in the scalar curvature response derived explicitly from the trace of the modified field equations. This produces a concrete phenomenological signature: a kernel-determined phase shift in interferometric measurements sensitive to curvature perturbations.

The construction therefore establishes a direct

$$\text{kernel} \;\rightarrow\; \text{response} \;\rightarrow\; \text{observable}$$

pipeline, enabling experimentally testable phenomenological constraints on history-dependent gravitational responses without reliance on strong-field, cosmological, or vacuum-propagation extrapolations.

This framework is presented as a minimal phenomenological curvature-memory extension of classical gravity. Its scope is limited and precise: to determine whether controlled, causal history dependence can be incorporated consistently into the geometric structure of GR while remaining empirically falsifiable.

Relation to Nonlocal and Modified-Gravity EFT Programs

Nonlocal modifications of gravity have a substantial literature, including infrared-motivated models in which inverse d'Alembertian operators or nonlocal form factors appear in the effective action (see, e.g., [10] and references therein), as well as local higher-curvature EFT corrections and modified-gravity frameworks such as $f(R)$ and scalar–tensor theories [11, 12, 13, 14].

The present framework differs in both construction and scope. First, the modification is formulated as a strictly retarded Volterra functional with explicit past-light-cone support, rather than through inverse differential operators or acausal Green-function structures.

Second, the observable sector is explicitly restricted to matter-coupled curvature response derived from the trace of the modified field equations. No independent scalar propagating mode is introduced in vacuum, and the vacuum graviton sector remains unmodified.

Third, the construction is organized within a small-coupling effective expansion with exact recovery of GR as $\alpha_0 \to 0$. The scalar realization presented here represents the leading operator in a systematic curvature–memory EFT hierarchy.

Accordingly, the present framework is best interpreted as a controlled, response-theoretic parameterization of curvature-memory effects within classical gravity, rather than as a specific infrared completion or a fundamental modification of the Einstein equations.

From a phenomenological perspective, the formulation developed here is designed to admit direct laboratory-scale tests. In contrast to many nonlocal gravity proposals that primarily target cosmological dynamics, the kernel-based response formalism provides a compact description of possible time-nonlocal curvature dynamics while preserving the general-relativistic limit. The resulting model leads to a specific observable prediction: a measurable phase-lag signal in precision interferometric measurements of gravitational acceleration. This phenomenological viewpoint allows the parameters $(\alpha_{\rm eff}, \tau)$ to be constrained experimentally without requiring commitment to a particular microscopic completion.

A further motivation for the Volterra kernel structure arises from linear response theory. In effective descriptions of many-body and continuum systems, the most general causal response of an observable to a driving source can be written as a retarded convolution with an admissible kernel. The Volterra form adopted here therefore represents the minimal causal generalization of an instantaneous constitutive relation. In this sense, the curvature–memory sector introduced in Eq. (2) can be interpreted as the leading response-theoretic extension of the local curvature–matter coupling encoded in Einstein's equations. The goal of the present work is therefore not to provide definitive experimental constraints, but to establish a mathematically consistent curvature–memory extension of classical gravity together with a closed observable pipeline that enables direct laboratory tests.

An important structural feature of the present construction is that the memory kernel acts only in the sourced curvature-response sector rather than in the propagating gravitational degrees of freedom. The vacuum Einstein equations and the transverse–traceless graviton sector therefore remain unchanged. The curvature–memory kernel may thus be interpreted as a response-theoretic generalization of the local curvature–matter constitutive relation in Einstein's equations, analogous to constitutive kernels in continuum response theory.

Contributions of this work. The purpose of the present work is to establish a minimal and internally consistent framework for curvature–memory response within an effective field theory description of classical gravity. Relative to existing nonlocal or modified-gravity constructions, the framework developed here provides three concrete elements.

First, a variational formulation in which a strictly causal Volterra-type curvature functional is incorporated directly into the gravitational action while preserving diffeomorphism invariance and exact recovery of the general-relativistic limit.

Second, a controlled linearized reduction that isolates the matter-coupled scalar curvature sector and yields a tractable non-Markovian response equation with well-defined perturbative control.

Third, an explicit kernel $\rightarrow$ response $\rightarrow$ observable pipeline linking the curvature-memory dynamics to experimentally measurable interferometric phase signals. This provides a concrete phenomenological parameterization of history-dependent gravitational response in laboratory-scale sourced configurations.

The present work therefore establishes the mathematical and phenomenological scaffolding required to analyze curvature-memory effects and to formulate experimentally testable response models, even though a unique observational discriminator between geometric and effective matter-sector memory lies beyond the scope of the linear-order framework developed here.

Conventions

We work in units $c = \hbar = 1$. The metric signature is $(-,+,+,+)$. Greek indices $\mu, \nu, \ldots$ run over spacetime coordinates. Covariant derivatives are defined with respect to the Levi–Civita connection of $g_{\mu\nu}$. Fourier transforms are defined by

$$\tilde{f}(\omega) = \int_{-\infty}^{\infty} f(t) e^{i\omega t} dt, \qquad f(t) = \frac{1}{2\pi} \int_{-\infty}^{\infty} \tilde{f}(\omega) e^{-i\omega t} d\omega.$$

The causal past of a point x is denoted $J^-(x)$. We assume perturbations vanish sufficiently rapidly as $t \rightarrow -\infty$, ensuring the existence of Fourier transforms and eliminating boundary terms under integration by parts.

2 Foundational Setup

Covariant Curvature–Memory Extension

Framework Core Statement. Within an effective field theory description of classical gravity, the geometric response sector may admit a causal, kernel-regulated dependence on prior curvature configurations, in addition to the instantaneous response to stress–energy described by Einstein's field equations.

More precisely, we posit that the effective curvature response can include temporally non-Markovian contributions constructed from admissible Volterra-

type memory kernels acting on curvature invariants. These contributions are required to satisfy:

1. **Covariance.** All memory terms are formulated in a fully diffeomorphism-invariant manner.
2. **Causality.** Memory kernels have support only within the past light cone of each spacetime point.
3. **Stability and Passivity.** Kernel admissibility conditions ensure well-posed integro-differential evolution and exclude acausal amplification.
4. **Exact GR Limit.** In the vanishing-memory limit, the modified field equations reduce exactly to Einstein's equations.

This curvature–memory coupling framework is formulated as a minimal phenomenological extension of classical gravity, restricted to a controlled, matter-coupled regime. No new matter fields, propagating gravitational degrees of freedom, or additional spacetime dimensions are introduced. Deviations from general relativity are controlled by a small set of parameters governing memory strength and relaxation timescale.

The purpose of this foundational construction is limited and precise: to determine whether history-dependent curvature–memory coupling can be incorporated consistently into the variational structure of GR while preserving conservation laws and yielding experimentally testable deviations in controlled regimes.

The formal realization of this framework proceeds by augmenting the Einstein–Hilbert action with causal, kernel-regulated curvature terms, leading to modified field equations that continuously recover GR in the appropriate limit.

3 Formal Construction: Minimal Scalar Memory Model

We construct this curvature–memory coupling framework with a kernel-regulated response within an effective field theory description of classical gravity, allowing the geometric response sector to include a controlled, causal non-Markovian correction. The starting point is the Einstein–Hilbert action

$$S_{\mathrm{EH}}[g] = \frac{1}{16\pi G}\int d^4x\,\sqrt{-g}\,(R - 2\Lambda_0). \tag{1}$$

where R is the Ricci scalar and Λ_0 is a baseline curvature offset.

Memory Sector

In an effective field theory context, such terms are introduced as symmetry-allowed curvature-response operators organized within a controlled derivative and coupling expansion, without commitment to a specific microscopic completion.

To introduce curvature memory while preserving diffeomorphism invariance, we augment the action by a minimal quadratic Volterra-type functional built from an admissible causal kernel:

$$S_{\rm mem} = \frac{\alpha_0}{2} \int d^4x \, \sqrt{-g(x)} \int_{\mathcal{J}^-(x)} d^4x' \, \sqrt{-g(x')} \, K_C(x,x') \, R(x) \, R(x') \quad (2)$$

Here α_0 is a dimensionless memory-coupling parameter and $\mathcal{J}^-(x)$ denotes the causal past of x.

The total action is

$$S[g,\Psi] = S_{\rm EH}[g] + S_{\rm mem}[g] + S_{\rm matt}[g,\Psi]. \quad (3)$$

Kernel Admissibility

The kernel $K_C(x,x')$ is assumed to satisfy standard admissibility conditions: (i) **causality**, $K_C(x,x') = 0$ for $x' \notin \mathcal{J}^-(x)$; (ii) **passivity/positivity** in frequency space (e.g. $\Re\, \widehat{K}_C(\omega) \geq 0$ in the reduced scalar model); and (iii) **decay** sufficient to ensure a well-posed integro-differential evolution. Exponential and fractional kernels provide representative admissible classes.

Justification of admissibility conditions. The causal (Volterra) structure ensures that the modified equations remain retarded integro–differential equations: the metric at a point depends only on past data within its light-cone. Standard results for Volterra operators imply that such systems admit well-posed initial-value formulations under sufficient decay conditions on the kernel. A detailed proof of well-posedness for specific kernel classes is beyond the scope of the present work. However, retarded Volterra-type integro–differential systems with sufficiently decaying kernels are known to admit well-posed initial-value formulations under standard functional-analytic conditions. The admissibility criteria imposed here are chosen precisely to place the curvature–memory sector within this well-behaved class of causal response operators.

The passivity condition $\Re\, \widehat{K}_C(\omega) \geq 0$ guarantees that the memory sector does not inject net energy into the system in linear response. In the frequency domain, this condition prevents the effective response denominator $1 + i\,\alpha_0\,\omega\,\widehat{K}_C(\omega)$ from developing runaway poles with positive real growth rates when $\alpha_0 > 0$, thereby excluding acausal exponential amplification in the small-coupling regime.

Sufficient temporal decay of $K_C(t)$ ensures that accumulated memory contributions remain finite and that the corresponding convolution operator is bounded on physically relevant function spaces. Together, these conditions restrict the theory to stable, causal, and perturbatively well-defined curvature–memory extensions of general relativity [3, 4, 5, 6].

Relation between α_0 and $\alpha_{\rm eff}$. The parameter α_0 appearing in the action Eq. (2) represents the fundamental dimensionless curvature–memory coupling parameter in the covariant theory. In the reduced scalar response sector derived

below, the observable response is controlled by an effective coupling $\alpha_{\rm eff}$ obtained after projection onto the matter-coupled scalar curvature sector and specialization to the near-field laboratory configuration.

The parameter $\alpha_{\rm eff}$ therefore represents the experimentally accessible coupling controlling the linear response amplitude in the reduced model. In general, $\alpha_{\rm eff}$ may differ from α_0 by order-unity geometric and projection factors associated with the scalar reduction and source configuration. Throughout the phenomenological analysis we treat $\alpha_{\rm eff}$ as the experimentally constrained parameter.

Well-posedness sketch for the exponential kernel (scalar sector). In the reduced scalar response model,

$$\delta\kappa(t) + \alpha_{\rm eff} \int_{-\infty}^{t} K_C(t-t') \, \frac{d}{dt'} \delta\kappa(t') \, dt' = \chi \, \delta p(t), \tag{4}$$

where $\delta\kappa \equiv \delta R$ denotes the scalar curvature perturbation obtained from the trace projection of the linearized field equations derived later in Section 5.1, and $\chi \equiv -8\pi G$ denotes the GR scalar curvature susceptibility relating the trace source δp to the curvature perturbation. The reduced scalar response form is introduced here only to establish well-posedness of the exponential kernel; its explicit derivation from the trace-projected dynamics is given in the later scalar reduction analysis.

The exponential kernel $K_C(t) = \tau^{-1} e^{-t/\tau} H(t)$ then yields $\widehat{K}_C(\omega) = (1 + i\omega\tau)^{-1}$ and hence an effective susceptibility

$$\chi_{\rm eff}(\omega) = \frac{\chi}{1 + i\alpha_{\rm eff}\omega \widehat{K}_C(\omega)}. \tag{5}$$

For $\alpha_{\rm eff} > 0$ the denominator has no poles with $\Im(\omega) > 0$ (equivalently, no exponentially growing modes in time) because the passivity condition $\Re \, \widehat{K}_C(\omega) \geq 0$ prevents the response factor $1 + i\alpha_{\rm eff}\omega \widehat{K}_C(\omega)$ from vanishing in the upper half-plane. Thus the exponential-kernel scalar sector is stable in linear response and admits a standard causal retarded Green-function formulation.

EFT interpretation of the memory kernel. Within the effective-field-theory viewpoint adopted here, the curvature–memory kernel should be interpreted as a phenomenological response operator parameterizing possible history-dependent corrections to the local curvature–matter constitutive relation. As in many EFT applications, the dimensionless coupling α_0 represents an effective coarse-grained response coefficient rather than a parameter fixed by a specific microscopic completion. Its magnitude must therefore be constrained empirically through experiment rather than predicted *a priori* by the present framework.

Retarded Volterra structure versus generic nonlocality. The present construction differs from generic nonlocal gravity models in which inverse differential operators (e.g. $\Box^{-1}$) or nonlocal form factors are introduced without

explicit retarded restriction. Here the memory sector is formulated as a *Volterra-type retarded functional* with support confined strictly to the past light cone of each spacetime point. Accordingly, the modification is organized as a causal history-dependent response rather than as a modification of the fundamental propagator or the introduction of acausal Green-function structures.

3.1 Field Equations

The memory contribution is defined variationally by

$$\mathcal{M}_{\mu\nu}[K_C] \equiv -\frac{2}{\sqrt{-g}}\frac{\delta S_{\rm mem}}{\delta g^{\mu\nu}}. \tag{6}$$

3.1.1 Variation of the Memory Action

Define the causal curvature functional

$$\mathcal{R}_C(x) \;\equiv\; \int_{J^-(x)} d^4x'\,\sqrt{-g(x')}\,K_C(x,x')\,R(x'), \tag{7}$$

so that the memory action in Eq. (2) can be written compactly as

$$S_{\rm mem} = \frac{\alpha_0}{2}\int d^4x\,\sqrt{-g(x)}\,R(x)\,\mathcal{R}_C(x). \tag{8}$$

Varying with respect to $g^{\mu\nu}$ gives

$$\delta S_{\rm mem} = \frac{\alpha_0}{2}\int d^4x\,\Big[\delta\big(\sqrt{-g}\,R\big)\;\mathcal{R}_C + \sqrt{-g}\,R\,\delta\mathcal{R}_C\Big]. \tag{9}$$

Using the standard identity (up to boundary terms)

$$\delta(\sqrt{-g}\,R) = \sqrt{-g}\,[G_{\mu\nu}\,\delta g^{\mu\nu} + (g_{\mu\nu}\Box - \nabla_\mu\nabla_\nu)\,\delta g^{\mu\nu}]\,, \tag{10}$$

integration by parts yields the explicit local-operator contribution

$$\begin{aligned}\delta S_{\rm mem} = \frac{\alpha_0}{2}\int d^4x\,\sqrt{-g}\;[\mathcal{R}_C\,G_{\mu\nu} + (g_{\mu\nu}\Box - \nabla_\mu\nabla_\nu)\,\mathcal{R}_C]\,\delta g^{\mu\nu}\\ + \frac{\alpha_0}{2}\int d^4x\,\sqrt{-g}\,R\,\delta\mathcal{R}_C.\end{aligned} \tag{11}$$

The remaining term $\delta\mathcal{R}_C$ contains the nonlocal metric variation through $\delta(\sqrt{-g'}R')$ and any implicit metric dependence of K_C and the causal domain $J^-(x)$. In the minimal EFT realization adopted here, we treat K_C as a fixed admissible causal kernel and retain the dominant contribution arising from δR within $\delta\mathcal{R}_C$. To this order, the memory contribution to the field equations can be written in a compact explicit form,

$$M_{\mu\nu}[K_C] = \alpha_0\,[\mathcal{R}_C\,G_{\mu\nu} + (g_{\mu\nu}\Box - \nabla_\mu\nabla_\nu)\,\mathcal{R}_C] \;+\; \Delta M_{\mu\nu}, \tag{12}$$

where $\Delta M_{\mu\nu}$ collects subleading terms from the full functional variation of $\mathcal{R}_C$ (including δK_C and the variation of the causal restriction). These terms are consistent with diffeomorphism invariance and the retarded Volterra structure, and may be incorporated systematically at higher order within the same effective expansion.

Effective field theory interpretation of $\Delta M_{\mu\nu}$. The tensor $\Delta M_{\mu\nu}$ collects contributions arising from (i) variations of the primed metric dependence inside $\mathcal{R}_C(x)$, (ii) any implicit metric dependence of the kernel $K_C(x, x')$, and (iii) variations of the causal restriction. In a symmetry-based effective field theory framework, such terms correspond to higher-order operators consistent with diffeomorphism invariance and the causal Volterra structure.

In the weak-curvature, small-coupling regime relevant to the phenomenological sector ($|R|L^2 \ll 1$ and $\alpha_0 \ll 1$), these additional contributions are parametrically suppressed relative to the leading retarded response terms retained in Eq. (12). They renormalize subleading curvature-memory operators in the same symmetry class without introducing new propagating degrees of freedom.

Accordingly, the present construction represents the lowest-order term in a systematic curvature-memory effective expansion. The falsifiable scalar response sector derived below is controlled entirely by the leading $\mathcal{O}(\alpha_0)$ retarded contribution, and is therefore insensitive to the detailed structure of $\Delta M_{\mu\nu}$ at this order.

This organization parallels the treatment of higher-curvature terms in gravitational effective field theory, where only the leading operators relevant to a specified observable sector are retained at a given order.

3.1.2 Modified Field Equations

Variation with respect to $g^{\mu\nu}$ yields modified field equations

$$G_{\mu\nu} + \Lambda_0 g_{\mu\nu} + \mathcal{M}_{\mu\nu}[K_C] = 8\pi G\, T_{\mu\nu} \tag{13}$$

where $\mathcal{M}_{\mu\nu}[K_C]$ is given explicitly by Eq. (12) in terms of the causal curvature functional $\mathcal{R}_C$ defined in Eq. (7).

By construction,

$$\lim_{\alpha_0 \to 0} \mathcal{M}_{\mu\nu}[K_C] = 0, \tag{14}$$

so that Eq. (13) reduces exactly to Einstein's equations.

Because the total action is diffeomorphism invariant, the total effective stress–energy is covariantly conserved [15]. Defining $T^{\rm mem}_{\mu\nu} \equiv -(8\pi G)^{-1}\mathcal{M}_{\mu\nu}[K_C]$, one has

$$\nabla^\mu \big(T_{\mu\nu} + T^{\rm mem}_{\mu\nu}\big) = 0, \tag{15}$$

ensuring compatibility with local conservation laws.

3.2 Minimal Scalar Realization and Tensor Structure

Having established the general form of the modified field equations, we now specify the minimal curvature–memory realization used in the phenomenological analysis.

In full generality, a covariant non-Markovian extension of the Einstein–Hilbert action may involve tensorial memory structures constructed from curvature tensors such as $R_{\mu\nu}$ or $R_{\mu\nu\rho\sigma}$, with corresponding index contractions inside the causal kernel.

In the present work, we restrict attention to the minimal scalar realization in which the memory sector is constructed solely from the Ricci scalar R. This choice preserves full covariance while avoiding the introduction of additional propagating tensor degrees of freedom and keeping the effective parameter space minimal. In particular, within the matter-coupled regime of interest, the Ricci scalar directly reflects local stress–energy via the GR trace relation $R = -8\pi GT$, ensuring that the scalar memory sector modifies sourced curvature response rather than vacuum gravitational wave propagation.

More general tensorial memory couplings are possible within the same variational framework but are not pursued here, as the scalar realization suffices to demonstrate the existence of a well-defined, causal curvature–memory sector and its associated observable consequences.

4 Linearized Non-Markovian Curvature Dynamics

We analyze the minimal scalar–memory model in the weak-field regime about Minkowski spacetime,

$$g_{\mu\nu} = \eta_{\mu\nu} + h_{\mu\nu}, \qquad |h_{\mu\nu}| \ll 1. \tag{16}$$

For calculational convenience, we may adopt transverse–traceless (TT) gauge when analyzing metric perturbations about Minkowski spacetime,

$$\partial^\mu h_{\mu\nu} = 0, \qquad h^\mu{}_\mu = 0, \tag{17}$$

while emphasizing that the observable sector studied below is obtained from the traced field equations in matter-coupled regimes rather than from vacuum TT gravitational-wave propagation. In this gauge, the linearized Einstein–Hilbert sector yields

$$\Box h_{\mu\nu} = -16\pi G\, T_{\mu\nu}. \tag{18}$$

4.1 Linearized Curvature Response

To connect the covariant field equations to the observable sector, we linearize about a background metric

$$g_{\mu\nu} = \bar{g}_{\mu\nu} + h_{\mu\nu}, \qquad |h_{\mu\nu}| \ll 1. \tag{19}$$

To leading order, the Ricci scalar perturbation satisfies

$$\delta R \sim \bar{\nabla}^2 h + \text{gauge terms}, \tag{20}$$

so that curvature perturbations are linear differential operators acting on $h_{\mu\nu}$.

Linearizing the memory functional defined in Eq. (7) gives

$$\delta\mathcal{R}_C(x) = \int_{J^-(x)} d^4x' \, \sqrt{-\bar{g}(x')}\, K_C(x, x')\, \delta R(x'). \tag{21}$$

Variation of the tensor structure $(g_{\mu\nu}\Box - \nabla_\mu\nabla_\nu)R$ appearing in the memory sector generates the same background differential operators acting on the linearized curvature perturbation.

Substituting into Eq. (12) and retaining only first-order terms in $h_{\mu\nu}$ yields a linear integro-differential equation of the form

$$\delta G_{\mu\nu}(x) + \alpha_0 \int_{J^-(x)} d^4x' \, K_C(x, x')\, \mathcal{D}_{\mu\nu}\, \delta R(x') = 8\pi G\, \delta T_{\mu\nu}(x), \tag{22}$$

where $\mathcal{D}_{\mu\nu}$ denotes the background differential operators arising from the $(g_{\mu\nu}\Box - \nabla_\mu\nabla_\nu)$ structure.

Scalar projection used for the phenomenological sector. Equation (22) is a tensor integro–differential relation. To isolate a minimal falsifiable sector without introducing additional propagating degrees of freedom, we project onto a curvature invariant by taking the scalar channel $\delta\kappa \equiv \delta R$, i.e. the trace/curvature sector generated at leading order by second derivatives of $h_{\mu\nu}$. This projection preserves covariance at the level of the invariant being modeled and captures the retarded response structure responsible for the phase lag analyzed in Section 5.

In the weak-field, locally inertial limit, the dominant structure may be captured by a representative scalar curvature perturbation $\delta\kappa$ driven by an effective source δp. The resulting causal Volterra response relation is developed explicitly in Section 5.1 Eq. (30).

In the weak-field regime about Minkowski spacetime, the dominant dynamical content of the memory sector enters through second-derivative curvature invariants. The scalar projection isolates this sector without introducing additional propagating tensor modes, and therefore captures the leading dispersive modification responsible for the frequency-dependent phase structure derived below.

4.2 Vacuum vs. Non-Vacuum Regime

The observable signal considered in the present phenomenological reduction arises in a matter-coupled near-field regime rather than in vacuum gravitational-wave propagation. In linearized general relativity about Minkowski spacetime, the Ricci scalar vanishes identically in vacuum and in transverse–traceless (TT) gauge, since $R_{\mu\nu} = 0$ implies $R = 0$ on shell. Accordingly, the scalar curvature

perturbation δR does not represent an independent propagating degree of freedom in vacuum gravitational-wave solutions.

The scalar sector analyzed here is therefore to be interpreted in a non-vacuum or near-source regime where $T_{\mu\nu} \neq 0$. At linear order the trace of Einstein's equations gives

$$\delta R \sim -8\pi G\, \delta T,$$

so that δR captures the effective curvature response generated by matter sources. In this setting the scalar curvature provides a controlled sector in which to probe possible history-dependent gravitational responses.

The present work does not claim any modification of vacuum gravitational-wave propagation. By construction, the framework does not introduce additional propagating gravitational degrees of freedom. Instead, the curvature–memory effect appears only in sourced configurations where the curvature response of the geometry can be probed through controlled matter perturbations. This restriction is phenomenologically useful because it allows laboratory-scale experiments—such as modulated mass distributions or interferometric measurements of gravitational acceleration—to probe the predicted response structure without requiring astrophysical strong-field environments.

Explicit trace projection to the scalar sector. To make the scalar reduction explicit, we contract Eq. (22) with the background metric $\bar{g}^{\mu\nu}$. Using

$$\bar{g}^{\mu\nu}\, \delta G_{\mu\nu} = -\,\delta R \tag{23}$$

at linear order, and noting that

$$\bar{g}^{\mu\nu}\, \mathcal{D}_{\mu\nu}\, \delta R = \bar{g}^{\mu\nu}\, (g_{\mu\nu}\Box - \nabla_\mu \nabla_\nu)\, \delta R = 3\, \Box\, \delta R \tag{24}$$

in four spacetime dimensions, the trace of Eq. (22) yields

$$-\,\delta R + 3\alpha_0 \int_{J^-(x)} d^4x'\, K_C(x, x')\, \Box\, \delta R(x') = 8\pi G\, \delta T, \tag{25}$$

where $\delta T = \bar{g}^{\mu\nu} \delta T_{\mu\nu}$.

To obtain the reduced one-dimensional retarded response form used in the phenomenological sector, we specialize to a locally inertial frame in a near-source region and consider perturbations whose spatial gradients are subdominant on the scale of the apparatus. In this approximation

$$\Box \simeq -\partial_t^2 \qquad (c = 1).$$

Substituting into Eq. (25) produces a memory term of the form

$$\int_{-\infty}^{t} K_C(t - t')\, \partial_{t'}^2 \delta R(t')\, dt'.$$

Assuming that δR and its first derivative vanish sufficiently rapidly as $t' \to -\infty$, integration by parts in t' yields the equivalent first-derivative Volterra operator

$$\int_{-\infty}^{t} K_C(t-t')\,\partial_{t'}\delta R(t')\,dt',$$

up to boundary terms. Defining $\delta\kappa \equiv \delta R$ then leads to the scalar response equation (30).

The boundary term $K_C(0)\,\partial_t \delta R(t)$ vanishes for perturbations that are switched on adiabatically or for stationary periodic driving, which we assume in the linear-response analysis in Section 5.

4.3 Geometric-response interpretation versus matter-sector memory

A potential interpretive question is whether the present construction is operationally distinguishable from introducing non-Markovian response directly in the matter sector, particularly in the reduced scalar regime where, at leading order in linearized GR, one has $\delta R \sim -8\pi G\,\delta T$ in non-vacuum configurations.

The distinction is that the memory kernel in the present framework is introduced at the level of the gravitational action through the curvature functional $S_{\rm mem}[g]$, and therefore modifies the geometric response side of the field equations rather than the matter action or the matter equations of motion. In this sense, the framework is not constructed as a constitutive law for stress–energy, but as a causal constitutive extension of the curvature response itself.

In the reduced scalar phenomenological sector, the sourced relation between δR and δT allows the memory effect to be probed experimentally through matter-coupled observables. However, the frequency-dependent phase lag arises from the retarded response kernel appearing in the curvature dynamics, i.e. on the left-hand side of the modified field equations, rather than from an assumed delay in the source sector. The present framework should therefore be interpreted as a modification of the geometry-to-source response relation, even though its experimentally accessible realization is necessarily matter-coupled in the scalar sector studied here.

A complete operational separation between geometric curvature memory and a more general non-Markovian effective matter description would require comparing the present construction to explicit matter-sector memory models, which lies beyond the scope of the present work. The claim made here is narrower: that a causal Volterra-type memory term can be consistently introduced in the geometric action and yields a distinct, falsifiable response structure in the sourced curvature sector.

4.4 Geometric–Matter Response Degeneracy at Linear Order

In effective descriptions of modified gravity, it is common for history-dependent response terms to be representable either on the geometric side of the field equations or within an effective matter-sector constitutive relation. Accordingly, one should expect a potential observational degeneracy between these descriptions at leading perturbative order.

At linear order in perturbations about a weak-field background, the modified curvature response derived here may therefore be observationally degenerate with an equivalent history-dependent response in the matter sector.

Specifically, in the non-vacuum linearized regime the trace of Einstein's equations yields

$$\delta R \approx -8\pi G\, \delta T. \tag{26}$$

A nonlocal response applied to curvature can therefore be written as

$$R(t) = R_{\mathrm{inst}}(t) + \alpha_{\mathrm{eff}} \int_0^\infty K(t-t')\, R_{\mathrm{inst}}(t')\, dt', \tag{27}$$

which produces the same leading-order observable behavior as an effective matter-sector response of the form

$$T(t) = T_{\mathrm{inst}}(t) + \alpha_{\mathrm{eff}} \int_0^\infty K(t-t')\, T_{\mathrm{inst}}(t')\, dt'. \tag{28}$$

Consequently, interferometric observables that depend only on the linear relation between curvature and stress–energy cannot uniquely distinguish whether the kernel-modified response is attributed to the geometric sector or to an effective matter coupling.

This degeneracy is common in effective descriptions of modified gravity, where field redefinitions or frame transformations can redistribute response terms between geometric and matter sectors without altering leading-order observables.

The framework presented here therefore defines a phenomenological test of history-dependent gravitational response in matter-coupled regimes. Distinguishing whether such response originates fundamentally from spacetime geometry or from effective matter coupling requires either higher-order curvature effects or additional observables sensitive to spatial gradients of the response.

5 Explicit Observable Pipeline

The minimal scalar-memory model predicts a frequency-dependent phase shift arising from causal curvature response. To make the kernel-to-observable map explicit, we express the linearized curvature dynamics as a retarded response relation.

Conventions. Throughout Section 5 we work in geometrized units with $c = 1$. Factors of c are restored only when converting the sourced trace perturbation δT (or $\delta\rho$) into laboratory units in the final scaling discussion.

5.1 Scalar Reduction and Effective Response

To connect the covariant linearized dynamics to a measurable response, we project Eq. (22) onto a representative scalar curvature perturbation. In the weak-field, locally inertial limit, the dominant dynamical content of the memory sector is captured by the linearized Ricci scalar perturbation,

$$\delta\kappa \equiv \delta R,$$

which is related to the metric perturbation by $\delta R \sim \partial^2 h$ at leading order.

Restricting attention to this scalar curvature invariant, which captures the second-derivative curvature sector responsible for the memory correction, and projecting Eq. (22) onto it, the traced and near-source–reduced dynamics take the scalar Volterra form.

We define the GR-normalized trace source

$$\delta p(t) \equiv \frac{\delta T(t)}{c^4} \;=\; \delta T(t) \qquad (c = 1). \tag{29}$$

Multiplying Eq. (25) by -1, defining $\delta\kappa \equiv \delta R$, absorbing the traced factor 3 into $\alpha_{\rm eff} \equiv 3\alpha_0$, and introducing the GR-normalized trace source $\delta p \equiv \delta T/c^4$ yields the reduced scalar Volterra equation

$$\delta\kappa(t) + \alpha_{\rm eff} \int_{-\infty}^{t} K_C(t-t')\,\frac{d}{dt'}\delta\kappa(t')\,dt' = -8\pi G\,\delta p(t), \tag{30}$$

where $\delta\kappa \equiv \delta R$. In the near-source reduction, the effective scalar memory coupling is

$$\alpha_{\rm eff} \equiv 3\alpha_0. \tag{31}$$

Matter-coupled source model. In the matter-coupled regimes emphasized here, $\delta p(t)$ denotes an effective scalar source for the curvature invariant $\delta\kappa \equiv \delta R$. A minimal example is a driven modulation of the local stress–energy trace, $\delta T(t, \mathbf{x})$, produced by an oscillating or time-modulated mass distribution in the vicinity of the readout region. To leading order in linearized GR one has $\delta R \sim -8\pi G\,\delta T$, so δp may be taken as a proxy for the controlled stress–energy modulation that drives the curvature response.

5.2 Frequency-Domain Response

Taking the Fourier transform of the causal convolution,

$$\mathcal{F}\left[\int_{-\infty}^{t} K_C(t-t')\,\frac{d}{dt'}\delta\kappa(t')\,dt'\right] = i\omega\,\widehat{K}_C(\omega)\,\widetilde{\delta\kappa}(\omega). \tag{32}$$

The causal Volterra convolution becomes multiplicative in frequency space.

Fourier transforming Eq. (30) yields

$$\widetilde{\delta\kappa}(\omega) = \chi_{\rm eff}(\omega)\,\widetilde{\delta p}(\omega) \tag{33}$$

with effective susceptibility

$$\chi_{\rm eff}(\omega) = \frac{-8\pi G}{1 + i\alpha_{\rm eff}\omega\widehat{K}_C(\omega)}. \tag{34}$$

The measurable quantity is the phase of the complex response:

$$\phi_{\rm mem}(\omega) = \arg[\chi_{\rm eff}(\omega)]\,. \tag{35}$$

A nonzero phase indicates a delayed curvature response relative to the driving perturbation.

Relation between curvature perturbations and local acceleration. In the weak-field, near-source regime relevant to laboratory experiments, the Ricci scalar perturbation δR is related to the Newtonian gravitational potential Φ through the linearized Einstein equations. For slowly varying sources,

$$\delta R \approx -2\nabla^2\Phi.$$

Since the local gravitational acceleration is

$$\delta a = -\nabla\Phi,$$

spatial integration over the apparatus scale yields an effective relation

$$\delta a(\omega) \propto L\,\delta\kappa(\omega),$$

where L denotes the characteristic spatial scale of the source–detector configuration. This provides the transfer relation connecting the curvature-response sector derived above to the acceleration observable measured by atom interferometers.

5.3 Explicit Exponential Kernel

For the admissible exponential kernel

$$K_C(t) = \frac{1}{\tau}e^{-t/\tau}H(t). \tag{36}$$

Its Fourier transform is

$$\widehat{K}_C(\omega) = \frac{1}{1 + i\omega\tau}. \tag{37}$$

Substituting into Eq. (34) gives

$$\chi_{\rm eff}(\omega) = \frac{-8\pi G}{1 + \frac{i\alpha_{\rm eff}\omega}{1+i\omega\tau}}. \tag{38}$$

The resulting phase lag is

$$\phi_{\rm mem}(\omega) = -\arctan\!\left(\frac{\alpha_{\rm eff}(\omega\tau)}{1 + (1+\alpha_{\rm eff})(\omega\tau)^2}\right). \tag{39}$$

Local dynamical realization for the exponential kernel. For the representative exponential kernel

$$K_C(t) = \tau^{-1} e^{-t/\tau} H(t),$$

the scalar Volterra equation

$$\delta\kappa(t) + \alpha_{\rm eff} \int_{-\infty}^{t} K_C(t-t')\, \frac{d}{dt'}\delta\kappa(t')\, dt' = \chi\, \delta p(t) \qquad (\chi = -8\pi G) \tag{40}$$

can be rewritten as a local first-order system by introducing an auxiliary memory variable

$$m(t) \equiv \int_{-\infty}^{t} K_C(t-t')\, \frac{d}{dt'}\delta\kappa(t')\, dt'. \tag{41}$$

For the exponential kernel, $m(t)$ satisfies

$$\tau\, \dot{m}(t) + m(t) = \dot{\delta\kappa}(t), \tag{42}$$

so that Eq. (40) becomes the coupled local system

$$\delta\kappa(t) + \alpha_{\rm eff}\, m(t) = \chi\, \delta p(t), \tag{43}$$

$$\tau\dot{m}(t) + m(t) = \dot{\delta\kappa}(t). \tag{44}$$

This representation shows explicitly that the exponential-kernel memory model is dynamically equivalent to a finite-dimensional retarded system with one additional auxiliary degree of freedom. For $\alpha_{\rm eff} > 0$ and $\tau > 0$, the homogeneous system admits no solutions with exponentially growing amplitude, since the characteristic polynomial has roots with non-positive real parts. Accordingly, the scalar exponential-kernel sector defines a well-posed initial-value problem with bounded retarded response. This auxiliary-variable representation parallels the standard treatment of Maxwell viscoelastic models in linear response theory.

5.4 Peak Response

The magnitude of the phase lag is maximized near

$$\omega\tau \sim 1, \tag{45}$$

corresponding to the transition between quasi-static ($\omega\tau \ll 1$) and rapidly oscillatory ($\omega\tau \gg 1$) regimes.

Instrument Transfer Function

The interferometric phase response can be expressed generically in frequency space as

$$\Delta\Phi_{\mathrm{AI}}(\omega) = \mathcal{T}(\omega, L)\, \delta a(\omega), \tag{46}$$

where $T(\omega, L)$ is the instrument transfer function determined by the interferometer pulse sequence, interrogation time, and baseline geometry. For light-pulse atom interferometers, $T(\omega, L)$ typically contains sinusoidal weighting factors encoding the temporal sampling of the acceleration field along the atomic trajectories.

Importantly, the curvature–memory prediction derived here affects the phase response through the frequency-dependent acceleration perturbation $\delta a(\omega)$. The resulting phase-lag signal therefore appears as a dispersive signature in $\Delta\Phi_{\mathrm{AI}}$ that is largely independent of the specific interferometer architecture, provided the instrument bandwidth overlaps the characteristic response scale $\omega \sim 1/\tau$.

The benchmark analysis presented below therefore treats $T(\omega, L)$ as an architecture-dependent weighting factor while focusing on the universal phase-lag signature produced by the curvature–memory kernel.

In a linearized readout, an interferometer measures a differential phase shift proportional to an external perturbation through an instrument-dependent transfer function $\mathcal{T}(\omega, L)$. High-precision optical and atom interferometers routinely achieve sub-milliradian phase resolution in laboratory settings (see, e.g., [16, 17]).

Substituting the curvature-induced acceleration perturbation derived in the previous section, the interferometer phase response can be written directly in terms of the curvature perturbation itself as

$$\Delta\Phi_{\mathrm{mem}}(\omega) = \mathcal{T}(\omega, L)\, \widetilde{\delta\kappa}(\omega). \tag{47}$$

Thus the measured phase acquires a frequency-dependent memory-induced lag $\phi_{\mathrm{mem}}(\omega)$.

As an illustrative matter-coupled configuration, consider an interferometric readout operated in the near-field of a modulated mass distribution, so that $\delta T(t) \neq 0$ in the region controlling the effective curvature response. In this setting, the phase readout is modeled as

$$\Delta\Phi_{\mathrm{mem}}(\omega) = \mathcal{T}(\omega)\, \widetilde{\delta\kappa}(\omega), \tag{48}$$

where $\mathcal{T}(\omega)$ encodes the instrument response to the local curvature perturbation (e.g., via an effective gravitational-gradient or potential-phase coupling in optical or atom interferometers). Atom interferometers have demonstrated high phase stability in precision inertial and gravitational measurements [16, 17], motivating their consideration as candidate architectures for matter-coupled curvature-response tests. The kernel-induced phase lag $\phi_{\mathrm{mem}}(\omega)$ is independent of the overall source amplitude and is maximized near $\omega\tau \sim 1$. A fully explicit numerical prediction for $\Delta\Phi_{\mathrm{mem}}$ requires specifying the sourced $\delta T(\omega)$ (or equivalently the

driven $\delta p(\omega) = \delta T(\omega)/c^4$ (restoring c)) and the instrument-specific $\mathcal{T}(\omega)$ for the chosen geometry.

Newtonian-limit link between δR and inertial acceleration. In the weak-field, slow-motion regime one may write $h_{00} = 2\Phi/c^2$, where Φ is the Newtonian potential. The spatial geodesic equation then reduces to $\mathbf{a} = -\nabla\Phi$. Moreover, Einstein's equations reduce to Poisson's equation $\nabla^2\Phi = 4\pi G\rho$. Combining this with the trace relation between the Ricci scalar and the (nonrelativistic) matter source implies $\nabla^2\Phi = -(c^2/2)\,\delta R$ (up to sign conventions). In spatial Fourier space this gives $\delta\mathbf{a}(\omega, \mathbf{k}) = -(c^2/2)\,(i\mathbf{k}/k^2)\,\delta R(\omega, \mathbf{k})$. Therefore any frequency-dependent susceptibility in the scalar curvature response $\delta R(\omega) = \chi_{\rm eff}(\omega)\,\delta p(\omega)$ induces the same complex response factor in Φ and in the measurable acceleration $\mathbf{a}$. Equivalently, the Newtonian sector behaves as if G is replaced by $G_{\rm eff}(\omega) = G\,[1 + i\alpha_{\rm eff}\omega\widehat{K}_C(\omega)]^{-1}$, so the memory-induced phase lag may be sought directly in the driven acceleration response.

5.5 Observable Mapping to Interferometric Phase

To connect the scalar-curvature response to an experimentally measurable signal, we consider the weak-field Newtonian limit of the metric perturbation. Writing the metric component as

$$g_{00} \simeq -(1 + 2\Phi/c^2), \tag{49}$$

the Newtonian potential Φ obeys

$$\nabla^2\delta\Phi = -\frac{c^2}{2}\,\delta R. \tag{50}$$

The resulting perturbation of the local gravitational acceleration is

$$\delta\mathbf{a} = -\nabla\delta\Phi. \tag{51}$$

A light-pulse atom interferometer measures acceleration along its sensitive axis $\hat{\mathbf{e}}$ through the standard phase response

$$\Delta\Phi_{\rm AI} \simeq k_{\rm eff}T^2\,\delta a_{\parallel}, \qquad \delta a_{\parallel} = \hat{\mathbf{e}}\cdot\delta\mathbf{a}, \tag{52}$$

where $k_{\rm eff}$ is the effective wavevector of the Raman pulses and T is the pulse separation time.

Equations (50)–(52) therefore establish the observable chain

$$\delta R \;\to\; \delta\Phi \;\to\; \delta a \;\to\; \Delta\Phi_{\rm AI},$$

showing explicitly how the curvature-memory response propagates into the interferometric phase observable.

This mapping provides the experimental readout channel used in the benchmark analysis below and should therefore be interpreted as an illustrative sensitivity study within the phenomenological parameter space $(\alpha_{\rm eff}, \tau)$ rather than as a prediction of a specific microscopic model.

5.6 Numerical Benchmark: Driven Source Mass Near an Atom Interferometer

To illustrate the magnitude of the predicted effect, we consider a concrete laboratory configuration consisting of a light-pulse atom interferometer operated near a harmonically modulated source mass.

Source configuration. Let a source mass M be positioned at mean distance r_0 from the interferometer and driven sinusoidally along the sensitive axis,

$$r(t) = r_0 + \Delta r \cos(\omega t), \qquad \Delta r \ll r_0.$$

The gravitational acceleration produced by the source mass is

$$a(t) = \frac{GM}{r(t)^2} = \frac{GM}{\big(r_0 + \Delta r \cos(\omega t)\big)^2}. \tag{53}$$

For small displacements $\Delta r/r_0 \ll 1$, a first-order Taylor expansion gives

$$a(t) \simeq \frac{GM}{r_0^2}\left[1 - 2\frac{\Delta r}{r_0}\cos(\omega t)\right] + \mathcal{O}\left(\frac{\Delta r}{r_0}\right)^2. \tag{54}$$

The oscillatory component therefore has amplitude

$$\delta a_0 \simeq 2\,\frac{\Delta r}{r_0}\,\frac{GM}{r_0^2}. \tag{55}$$

Choice of benchmark parameters. The representative values of the memory parameters used in the illustrative benchmark are not intended as fundamental predictions of the framework. In an effective-field-theory interpretation the parameters $(\alpha_{\rm eff}, \tau)$ are phenomenological response coefficients that must ultimately be constrained experimentally rather than fixed *a priori*. The benchmark values are therefore chosen to satisfy two practical requirements.

First, the scalar-memory correction should remain within a controlled perturbative regime. The frequency-domain response depends on the dimensionless parameter $\varepsilon(\omega) = \alpha_{\rm eff}\omega\tau$, so perturbative consistency requires $|\varepsilon| \ll 1$ in the measurement band. This motivates the use of small illustrative couplings $\alpha_{\rm eff} \lesssim 10^{-2}$.

Second, the memory-induced phase lag is maximized when the driving frequency satisfies $\omega\tau \sim 1$. In the laboratory benchmark considered here, the source mass is modulated at frequencies of order $f \sim 10$ Hz, corresponding to angular frequency $\omega = 2\pi f \sim 60\ \mathrm{rad\,s^{-1}}$. The peak-response condition $\omega\tau \sim 1$ therefore implies a characteristic relaxation timescale

$$\tau \sim \omega^{-1} \sim (2\pi f)^{-1} \sim 10^{-2}\ \mathrm{s}. \tag{56}$$

Thus the value $\tau \sim 10^{-2}$ s should be interpreted only as a representative benchmark within the experimentally accessible frequency band. The parameters $(\alpha_{\rm eff}, \tau)$ are treated as phenomenological response coefficients whose values

must ultimately be constrained by experiment rather than predicted by the present effective-field-theory description. The benchmark configuration therefore illustrates the region of $(\alpha_{\rm eff}, \tau)$ parameter space that could be probed by a laboratory-scale interferometric measurement operating in the frequency range considered here.

More generally, τ should be interpreted as an effective relaxation or correlation time associated with the coarse-grained gravitational response sector. Possible microscopic interpretations include the correlation time of an eliminated dynamical sector or a phenomenological response timescale in the sense of generalized Langevin descriptions of non-Markovian systems.

Representative parameters. We adopt the benchmark values

$$M = 100 \text{ kg}, \qquad r_0 = 0.20 \text{ m}, \qquad \Delta r = 0.01 \text{ m},$$

so that $\Delta r/r_0 = 0.05$ remains safely within the small-displacement regime.

Table 1: Representative benchmark parameters used in the illustrative interferometer configuration.

Parameter	Value
Source mass M	100 kg
Mean separation r_0	0.20 m
Oscillation amplitude Δr	0.01 m
Drive frequencies f	$\{1, 10, 100\}$ Hz
Interferometer wavevector $k_{\rm eff}$	1.6×10^7 m^{-1}
Pulse separation time T	0.50 s
Phase sensitivity σ_ϕ	10^{-3} rad

The ratio $\Delta r/r_0 = 0.05$ ensures that second-order corrections of order $(\Delta r/r_0)^2 \approx 2.5 \times 10^{-3}$ remain negligible for the purposes of the illustrative benchmark.

These values yield

$$\delta a_0 \approx 1.67 \times 10^{-8} \text{ m s}^{-2}. \tag{57}$$

For a representative light-pulse atom interferometer with effective wavevector $k_{\rm eff} = 1.6 \times 10^7$ m^{-1} and pulse separation time $T = 0.50$ s, the acceleration-induced phase amplitude is

$$|\Delta\Phi_0| \simeq k_{\rm eff} T^2 \delta a_0 \approx 0.0667 \text{ rad}. \tag{58}$$

Memory-induced phase lag. Using the exponential-kernel closed form in Eq. (39), and choosing representative memory parameters

$$\tau = 0.01 \text{ s}, \qquad \alpha_{\rm eff} = 2 \times 10^{-3},$$

the response transitions most strongly in the characteristic relaxation band $\omega\tau \sim 1$, corresponding to driving frequencies $f \sim 10$ Hz ($\omega \sim 10^2$ rad s^{-1}), well within the perturbative regime $\alpha_{\rm eff}\omega\tau \ll 1$. At this point,

$$\phi_{\rm mem} = -\arctan\left(\frac{\alpha_{\rm eff}}{2+\alpha_{\rm eff}}\right) \approx -1.0\times10^{-3}\ \text{rad} \approx -0.057^\circ. \tag{59}$$

This corresponds to an effective time delay

$$\Delta t = \frac{|\phi_{\rm mem}|}{\omega} \approx 1.0\times10^{-5}\ \text{s}. \tag{60}$$

Experimental implication. For the benchmark configuration above, the predicted interferometric signal is therefore

$$\Delta\Phi_{\rm mem}(t) \approx (0.0667\ \text{rad})\cos\big(\omega t + \phi_{\rm mem}\big), \tag{61}$$

with a measurable phase lag $|\phi_{\rm mem}| \sim 10^{-3}$ rad. An experiment capable of resolving phase at the 10^{-3} rad level would therefore probe couplings of order $\alpha_{\rm eff} \sim 10^{-3}$ in the regime $\omega\tau \sim 1$, corresponding to the peak-response condition $|\phi_{\rm mem}|_{\rm max} \sim \alpha_{\rm eff}/2$ for small coupling.

Experimental context. Modern light-pulse interferometers routinely achieve phase stability in the range $\sigma_\phi \sim 10^{-3}$–10^{-4} rad in precision measurements of gravitational acceleration and gradients. Such sensitivities have been demonstrated in laboratory interferometers developed for tests of Newtonian gravity and inertial sensing [16]. Proposed large-baseline instruments designed for precision gravitational measurements and dark-matter searches are expected to achieve comparable or improved phase resolution over similar frequency bands. Consequently, the benchmark sensitivity adopted here should be interpreted as representative of current or near-future experimental capability rather than an optimistic extrapolation.

Constraint interpretation. Experimental sensitivity is characterized by the phase-resolution threshold σ_ϕ of the interferometer. The absence of a detectable phase lag therefore implies the condition

$$|\phi_{\rm mem}(\omega;\alpha_{\rm eff},\tau)| \le \sigma_\phi. \tag{62}$$

In the small-coupling regime $\alpha_{\rm eff} \ll 1$, the exponential kernel yields the approximate phase lag

$$\phi_{\rm mem}(\omega) \simeq -\alpha_{\rm eff}\,\frac{\omega\tau}{1+(\omega\tau)^2}. \tag{63}$$

This leads to the exclusion condition

$$\alpha_{\rm eff} \lesssim \sigma_\phi\,\frac{1+(\omega\tau)^2}{\omega\tau}. \tag{64}$$

Equation (64) defines a curve in the parameter space $(\alpha_{\rm eff}, \tau)$ that can be probed by a driven-source atom-interferometer experiment operating at angular frequency ω. The strongest sensitivity occurs near the peak-response condition $\omega\tau \simeq 1$, where

$$\alpha_{\rm eff}^{\rm min} \simeq 2\sigma_\phi. \tag{65}$$

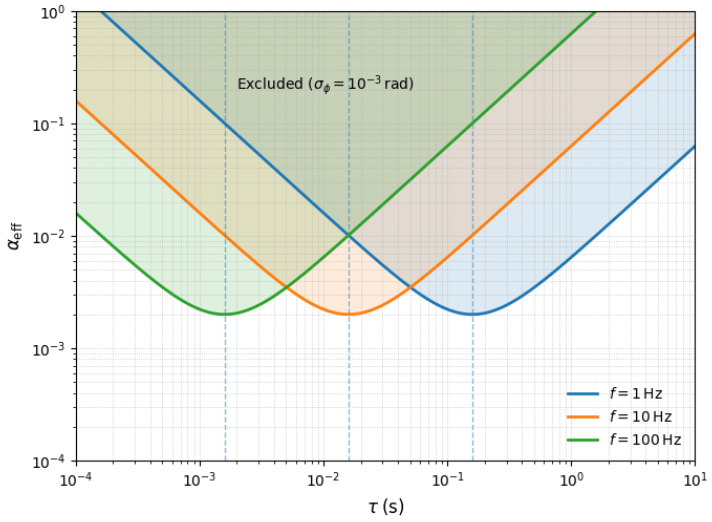

Figure 1: Exclusion curves in the parameter space $(\alpha_{\rm eff}, \tau)$ for a driven-source atom-interferometer experiment with phase sensitivity $\sigma_\phi = 10^{-3}$ rad. The curves correspond to representative drive frequencies $f = \{1, 10, 100\}$ Hz. The shaded region above each curve is excluded by a null result. Sensitivity is maximized near the peak-response condition $\omega\tau \simeq 1$, where the minimum detectable coupling is $\alpha_{\rm eff}^{\rm min} \simeq 2\sigma_\phi$.

Relation to existing experimental sensitivities. Current atom-interferometric measurements of gravitational acceleration provide a useful order-of-magnitude benchmark for the phase sensitivities relevant to the present framework. Early precision measurements using light-pulse atom interferometers achieved phase sensitivities at the $\sim 10^{-3}$–10^{-4} rad level in gravitational acceleration measurements [24]. Modern large-momentum-transfer and long-baseline interferometers have demonstrated sensitivities well below 10^{-3} rad in differential phase measurements.

In the curvature–memory framework developed here, the observable signal appears as a small phase lag relative to the instantaneous general-relativistic acceleration signal. For a representative near-field configuration producing a GR-scale phase amplitude $|\Delta\Phi_0| \sim 10^{-1}$ rad, a detectable memory-induced phase lag $\delta\Phi \sim 10^{-3}$ rad corresponds to a fractional response lag of order 10^{-2}. Within

the scalar response model, this translates to an effective coupling $\alpha_{\rm eff} \sim 10^{-3}$ when the system is tuned near the peak-response regime $\omega\tau \sim 1$.

These estimates indicate that existing interferometric measurements do not yet exclude the benchmark parameter region illustrated in the present analysis, but they demonstrate that history-dependent gravitational phase responses at the $\sim 10^{-3}$ rad level lie within the sensitivity range of current or near-future precision interferometry. The exclusion curves presented in this work therefore represent experimentally accessible parameter space rather than purely speculative regimes.

5.7 Consistency with existing laboratory tests

Existing laboratory tests of gravity place stringent constraints on deviations from Newtonian response and on possible fifth-force interactions. Precision torsion-balance experiments, such as the Eöt-Wash program, constrain static modifications of the gravitational potential at sub-meter scales with high sensitivity [22, 23]. In addition, modern atom interferometer experiments provide extremely precise measurements of local gravitational acceleration and have demonstrated sub-milliradian phase sensitivity in controlled laboratory settings [24, 25].

The curvature-memory framework considered here differs qualitatively from static potential modifications in that the predicted signal is a *frequency-dependent phase lag* in the curvature response rather than a static correction to the gravitational force law. The observable therefore appears as a dispersive response of the sourced curvature sector under time-dependent driving rather than as a change in the equilibrium gravitational potential.

Accordingly, existing static fifth-force constraints do not directly bound the parameter space $(\alpha_{\rm eff}, \tau)$ considered here. However, precision measurements of time-dependent gravitational signals—including interferometric measurements of modulated gravitational sources—may place bounds on the curvature–memory response parameters.

As a rough order-of-magnitude estimate, atom interferometers achieving phase sensitivities of $\sigma_\phi \sim 10^{-3}$ rad and operating at modulation frequencies $\omega \sim 10$–$100\ \mathrm{rad\,s^{-1}}$ would already be sensitive to couplings $\alpha_{\rm eff} \gtrsim 10^{-3}$ in the regime $\omega\tau \sim 1$. Consequently, the parameter space with $\alpha_{\rm eff} \gtrsim 10^{-3}$ and $\tau \sim 10^{-2}\,\mathrm{s}$ could be probed by laboratory-scale interferometric measurements, while smaller couplings remain unconstrained by present data. A systematic comparison with published experimental datasets is deferred to future work.

5.8 GR Limit

In the vanishing-memory limit $\alpha_{\rm eff} \to 0$ we obtain

$$\chi_{\rm eff}(\omega) \to \chi, \qquad \phi_{\rm mem}(\omega) \to 0, \tag{66}$$

so that the curvature response becomes instantaneous and the model reduces smoothly to classical general relativity.

5.9 Matter-Coupled Source Model and Observable Scaling

Restoring physical units. Restoring factors of c, the trace-sourced scalar curvature perturbation in linearized GR satisfies, to leading order,

$$\delta R \;\simeq\; -\frac{8\pi G}{c^4}\,\delta T. \tag{67}$$

For nonrelativistic matter, $\delta T \simeq c^2\delta\rho$, hence

$$\delta R \;\simeq\; -\frac{8\pi G}{c^2}\,\delta\rho. \tag{68}$$

Defining $\delta p \equiv \delta T/c^4$ recasts the source as $\delta R \simeq -8\pi G\,\delta p$, making explicit the normalization used in Section 5.

This relation provides a concrete identification of the driving perturbation in the scalar response model. Accordingly, the effective source in Eq. (30) may be interpreted as a controlled stress–energy modulation, with $\delta p(t) \propto \delta\rho(t)$ (or equivalently $\delta p \propto \delta T$), the proportionality absorbed into the susceptibility χ.

As a minimal laboratory realization, consider a driven source mass that produces a periodic density perturbation in a localized region near an optical interface (or near an atom-interferometer test mass), generating a harmonic curvature drive $\delta p(t) = \delta p_0 \cos(\omega t)$. In frequency space, the scalar Volterra response implies

$$\widetilde{\delta\kappa}(\omega) = \chi_{\rm eff}(\omega)\,\widetilde{\delta p}(\omega), \qquad \phi_{\rm mem}(\omega) = \arg[\chi_{\rm eff}(\omega)], \tag{69}$$

so that the observable phase shift inherits the memory-induced lag:

$$\Delta\Phi_{\rm mem}(\omega) = \mathcal{T}(\omega, L)\,\widetilde{\delta\kappa}(\omega) = \mathcal{T}(\omega, L)\,\chi_{\rm eff}(\omega)\,\widetilde{\delta p}(\omega). \tag{70}$$

At peak response $\omega\tau \sim 1$ and small $\alpha_{\rm eff}$, one has $|\phi_{\rm mem}|_{\max} \sim \alpha_{\rm eff}/2$, so the intrinsic memory-induced phase lag scales linearly with $\alpha_{\rm eff}$. Detectability then depends on the realized curvature-drive amplitude δp_0 and the specific transfer function $\mathcal{T}(\omega, L)$ of the chosen interferometric architecture. This formulation should therefore be read as providing an explicit *source-to-observable* scaling relation in matter-coupled regimes, rather than a claim of immediate detectability in any single existing instrument.

5.10 Candidate Experimental Geometries

The matter-coupled scalar memory sector considered here requires a controlled time-dependent stress–energy source in the vicinity of the measurement region. Several conceptually viable laboratory configurations include:

- An oscillating or modulated dense test mass placed near one arm of an interferometer, producing a periodic $\delta T(t)$ and corresponding curvature modulation.

- A driven cavity or mechanical resonator whose mass distribution is modulated at frequency $\omega \sim \tau^{-1}$, maximizing the phase-lag response in the scalar sector.
- Atom-interferometric geometries in which a nearby time-dependent gravitational potential source produces a controlled modulation of the local curvature invariant.

These configurations serve only as illustrative realizations of a matter-driven curvature response sector; detailed sensitivity forecasts depend on the specific mass distribution, distance scale, and instrumental transfer function.

Technical distinction from inverse-operator nonlocal gravity. Unlike constructions based on inverse differential operators (e.g. $\Box^{-1}$ acting on curvature scalars), the present framework does not introduce fundamental nonlocal operators or modify the vacuum graviton propagator. The memory sector is formulated as a strictly retarded Volterra functional with explicit past-light-cone support and small coupling α_0, and the observable sector is restricted to matter-coupled curvature response. In vacuum, no independent scalar propagating mode is introduced.

5.11 Structural Position Within Nonlocal EFT

The present framework is not intended as a unique nonlocal completion of general relativity. Instead it should be interpreted as a minimal causal response parameterization of possible curvature-memory effects within an effective field theory description of classical gravity, whose parameters may be constrained experimentally.

Possible microscopic origins of such response behavior are not specified within the present phenomenological framework. However, several known mechanisms in gravitational effective field theory naturally generate retarded or history-dependent interactions. Integrating out additional degrees of freedom or coarse-graining over unresolved sectors typically produces nonlocal response kernels in the resulting low-energy dynamics, a structure familiar from open-system and generalized Langevin descriptions. Related hereditary effects already appear in classical gravitational EFT through tail terms in post-Newtonian expansions, which encode the influence of prior curvature configurations on the present dynamics. The present model therefore should be interpreted as a minimal causal parameterization of such possible curvature-memory effects rather than as a specific microscopic completion.

Within the broader landscape of nonlocal gravitational EFTs, such response kernels provide a phenomenological way of capturing retarded or history-dependent geometric dynamics without committing to a specific microscopic completion.

In the benchmark analysis below we adopt the single-timescale exponential kernel derived in Section 5, corresponding to a Debye-type relaxation profile

in linear-response terminology. In the reduced scalar sector, the resulting susceptibility exhibits a smooth frequency-dependent phase lag

$$\phi(\omega) = \arctan(\omega\tau) - \arctan\big(\omega(\tau + \alpha_{\text{eff}})\big), \tag{71}$$

which vanishes in both the low- and high-frequency limits and peaks near $\omega \sim 1/\tau$.

Finite-Order Local Analytic EFT. Consider a finite-order local analytic expansion of the form

$$F(\Box) = c_0 + c_1\Box + c_2\Box^2 + \cdots + c_N\Box^N, \tag{72}$$

with real coefficients c_i. In the weak-field, $k \to 0$ scalar reduction, such operators generate polynomial frequency dependence in ω^2. The resulting linear response function remains purely real (modulo trivial π phase flips) in the absence of additional absorptive structure.

Accordingly, finite-order local analytic curvature corrections can reproduce low-frequency amplitude renormalization but *cannot reproduce the smooth Debye-type phase lag* characteristic of the retarded Volterra kernel.

Thus, the phase structure derived in the present model cleanly distinguishes the curvature–memory sector from purely local analytic EFT corrections.

Broader Nonlocal Admissible Form Factors. However, the space of admissible nonlocal EFT modifications is larger than the finite-order analytic subclass. Causal nonlocal form factors consistent with covariance, passivity, and Kramers–Kronig dispersion relations may generate dispersive response functions with nontrivial frequency-dependent phase structure.

In particular, non-analytic or infinite-order analytic form factors, or retarded curvature functionals constructed from completely monotone kernel families, can reproduce Debye-type response profiles within a consistent linear-response framework.

Therefore, while the present construction is structurally distinct from finite-order local analytic EFT corrections, it is *not mathematically unique within the full admissible nonlocal EFT space.*

Interpretive Position. The framework presented here should therefore be interpreted as:

- A minimal causal Volterra realization of curvature–memory response;
- A controlled, small-coupling, matter-coupled EFT sector;
- A concrete representative of admissible non-Markovian curvature dynamics;
- A model providing a clean kernel $\to$ response $\to$ observable pipeline.

The significance of the construction lies not in uniqueness of formal structure, but in:

1. The explicit restriction to strictly retarded Volterra form;
2. Exact recovery of GR in the vanishing-memory limit;
3. Absence of new propagating vacuum tensor modes;
4. A well-defined experimental discriminator within the matter-coupled scalar sector.

Accordingly, the present framework is best understood as a *minimal phenomenological representative of a broader admissible curvature-response sector*, rather than as a unique nonlocal completion of gravity.

5.12 Possible geometric–matter discrimination strategies

While the interferometric phase observable primarily probes the local gravitational acceleration, atom interferometer gradiometers measure spatial gradients of the acceleration field. Such instruments therefore provide sensitivity to spatial derivatives of the curvature response.

The discussion below should be interpreted as an illustrative extension of the linear-response framework developed in this paper. A fully quantitative treatment of geometric–matter discrimination using gradiometer configurations lies beyond the linear-order framework considered here.

Baseline–retardation criterion. A simple condition illustrates when gradient observables can distinguish geometric curvature memory from an effective matter-sector memory description.

Consider two spatially separated interferometers forming a gradiometer with baseline length L. In the geometric-memory model, the retarded curvature response propagates causally through the spacetime geometry, so the memory-modified curvature perturbation satisfies

$$\delta R(t,\mathbf{x}) = \int_{J^-(x)} K_C(t-t', |\mathbf{x}-\mathbf{x}'|)\, \delta T(t',\mathbf{x}')\, d^4x'. \tag{73}$$

As a result, the curvature response at the two interferometer locations differs by a retardation time of order

$$\Delta t_{\rm geom} \sim \frac{L}{c}. \tag{74}$$

In contrast, a purely matter-sector memory model introduces history dependence only in the source response,

$$T(t) = T_{\rm inst}(t) + \alpha_{\rm eff} \int_0^\infty K(t-t')\, T_{\rm inst}(t')\, dt', \tag{75}$$

so that the geometric propagation remains instantaneous at the level of the Newtonian field equation.

Consequently, the two models predict measurably different spatial gradient responses once the intrinsic kernel timescale becomes comparable to the light-travel time across the baseline,

$$\tau \gtrsim \frac{L}{c}. \tag{76}$$

For typical laboratory gradiometer baselines of $L \sim 1$–10 m, this criterion corresponds to $\tau \gtrsim 3 \times 10^{-9}$–$3 \times 10^{-8}$ s, well below the benchmark response timescale $\tau \sim 10^{-2}$ s considered in the illustrative analysis of Section 5.7.

When condition (76) is satisfied, the geometric-memory model produces a baseline-dependent phase lag in the gradiometer signal, while a matter-sector memory model produces only a local temporal response independent of L. Spatially separated interferometers therefore provide a potential experimental discriminator between geometric and effective matter-sector memory descriptions.

Detailed modeling of such gradiometer configurations lies beyond the scope of the present work, but this possibility illustrates that additional observables may allow the degeneracy between geometric and matter-sector memory to be experimentally broken.

Interpretive scope of the framework. The present construction should be interpreted as establishing a consistent phenomenological framework for curvature–memory response within an effective field theory description of classical gravity. At linear order in weak-field perturbations the resulting observable signal can be formally degenerate with an equivalent non-Markovian response introduced in the matter sector, as discussed in Section 4.4. The purpose of the present work is therefore not to claim a unique observational signature of geometric memory at this order, but rather to demonstrate that a causal curvature-memory functional can be consistently incorporated into the gravitational action and leads to a well-defined kernel $\rightarrow$ response $\rightarrow$ observable pipeline in matter-coupled regimes.

In this sense, the framework provides the mathematical and phenomenological scaffolding necessary for future investigations of history-dependent gravitational response. Distinguishing geometric curvature memory from effective matter-sector descriptions would require either higher-order curvature effects or additional observables sensitive to spatial propagation. Developing such discriminators lies beyond the scope of the present work.

5.13 Observable Pipeline and Experimental Signature

To summarize the phenomenological implications of the model, the construction closes the full observable pipeline from the curvature–memory kernel to experimentally measurable signals,

$$\delta R \;\rightarrow\; \delta a \;\rightarrow\; \Delta\Phi_{\mathrm{AI}},$$

linking the modified geometric response directly to interferometric phase measurements. This explicit mapping distinguishes the present framework from

many modified-gravity proposals in which the connection between theoretical modifications and laboratory observables remains indirect or cosmological in nature.

6 Discussion and Conclusion

In this work we have investigated whether the geometric response sector of classical gravity can consistently admit a small, causal history-dependent correction while preserving the core symmetries and empirical successes of general relativity.

We have constructed a minimal covariant extension of general relativity in which the effective curvature response may include a causal, kernel-regulated memory contribution. The formulation is entirely variational, preserves diffeomorphism invariance, and reduces exactly to Einstein's field equations in the vanishing-memory limit $\alpha_0 \to 0$.

The modification is controlled by a dimensionless coupling parameter α_0 and an admissible Volterra kernel K_C satisfying causality, passivity, and decay conditions. No new propagating tensor degrees of freedom are introduced, and the matter sector remains unchanged. All deviations from GR arise from the non-Markovian structure of the curvature sector, implemented through a retarded Volterra functional.

In the linearized, matter-coupled regime derived from the traced field equations, the principal phenomenological consequence is a frequency-dependent phase lag in the scalar curvature response. For the exponential-kernel example, the lag exhibits a characteristic scale set by $\omega\tau \sim 1$, providing a concrete experimental signature. For a specified matter-coupled source configuration and instrument response, the presence or absence of this phase lag is an experimentally decidable question. The framework is therefore falsifiable without reliance on cosmological or strong-field extrapolations.

Several limitations should be emphasized. First, the memory kernel is introduced at the level of an effective field theory as a causal, retarded curvature-response functional. The construction therefore functions as a controlled curvature extension valid within a specified weak-curvature, small-coupling regime ($\alpha_0 \ll 1$), without commitment to a specific microscopic completion. Second, the present analysis has been carried out primarily in the linearized sector; a full nonlinear stability analysis and exploration of strongly curved regimes remain open directions. Third, the scalar-memory model represents the minimal covariant realization sufficient to capture the leading matter-coupled curvature response; more general tensorial memory structures are possible within the same variational framework but are not required for the phenomenological sector developed here.

Within these constraints, the construction demonstrates that a consistent curvature–memory extension of the effective geometric response sector of general relativity can be formulated while preserving covariance and conservation laws. In this sense, the framework may be viewed as a phenomenological realization of a broader class of nonlocal gravitational effective field theories, in which retarded

kernels parameterize possible coarse-grained dynamics of spacetime geometry. Whether curvature exhibits measurable history dependence is ultimately an empirical question. The formulation presented here establishes a mathematically controlled and experimentally testable pathway for addressing that question.

Appendix — Perturbative Control, EFT Naturalness, and Experimental Reach for the Scalar Curvature–Memory Sector

This appendix provides the technical support for the benchmark phenomenology used in the main text, including perturbative-control estimates, EFT parameter interpretation, approximation accuracy, and observable-scaling relations. The derivations presented here justify the response model, approximation regime, and exclusion-curve construction used in Section 5.

Specifically, it addresses: (i) the regime of perturbative control of the scalar-memory response, (ii) the effective-field-theory interpretation of the parameters α_0 and τ, (iii) the accuracy of the small-coupling phase-lag approximation, (iv) the explicit observable chain $\delta R \to \delta\Phi \to \delta a \to \Delta\Phi_{\rm AI}$, and (v) the construction of exclusion curves in the $(\alpha_{\rm eff}, \tau)$ plane.

Overview of Perturbative Regime

The reduced scalar Volterra model used in the main text has the frequency-domain response

$$\chi_{\rm eff}(\omega) = \frac{\chi}{1 + i\,\alpha_{\rm eff}\,\omega\,\widehat{K}_C(\omega)}, \tag{77}$$

where χ denotes the static curvature–source response coefficient, which reduces to the general-relativistic trace relation $\chi = -8\pi G$ in the instantaneous-response limit.

The small parameter controlling perturbative response is therefore

$$\varepsilon(\omega) \equiv \alpha_{\rm eff}\,\omega\,\widehat{K}_C(\omega), \qquad |\varepsilon(\omega)| \ll 1. \tag{78}$$

For the exponential kernel, this reduces near the peak-response regime $\omega\tau \sim 1$ to the simple requirement

$$\alpha_{\rm eff} \ll 1. \tag{79}$$

Within the EFT interpretation adopted in the main text, neither α_0 nor τ is fixed uniquely without specifying a microscopic completion. Instead, they should be interpreted as phenomenological response parameters: α_0 is a Wilson-type coupling that must be bounded empirically, while τ is an effective relaxation or correlation time associated with the coarse-grained sector [3, 4, 18, 19].

For the exponential kernel, the leading-order phase approximation remains highly accurate for $\alpha_{\rm eff} \lesssim 10^{-3}$ and remains percent-level accurate near $\omega\tau \sim 1$ for $\alpha_{\rm eff} \sim 10^{-2}$. A conservative illustrative benchmark is therefore

$$\alpha_{\rm eff} \lesssim 10^{-2}. \tag{80}$$

A corrected near-field atom-interferometer benchmark with $\Delta r/r_0 \leq 0.05$ yields a GR-scale phase amplitude $|\Delta\Phi_0| \sim 0.07$ rad, while a detectable memory-induced phase lag at the 10^{-3} rad level corresponds to $\alpha_{\rm eff} \sim 2 \times 10^{-3}$ when tuned near $\omega\tau = 1$.

Finally, the appropriate exclusion statement is not a single point in parameter space but a curve:

$$|\phi_{\rm mem}(\omega; \alpha_{\rm eff}, \tau)| \leq \sigma_\phi, \tag{81}$$

which, in the small-coupling regime for the exponential kernel, becomes

$$\alpha_{\rm eff,max}(\tau; \sigma_\phi, \omega) \approx \sigma_\phi \, \frac{1 + (\omega\tau)^2}{\omega\tau}. \tag{82}$$

This reaches its minimum at $\omega\tau = 1$, where

$$\alpha^{\rm min}_{\rm eff,max} = 2\sigma_\phi. \tag{83}$$

A.1 Perturbative Control of the Scalar-Memory Response

Exact versus perturbative statements

The exponential-kernel expressions used in the main text are exact solutions of the reduced scalar Volterra model, given the scalar projection, near-source reduction, and chosen kernel family. The perturbative question is therefore not whether the closed-form expression is algebraically exact, but whether the retained scalar-memory sector constitutes a controlled small deformation of the GR response in the experimental band.

Starting from Eq. (77),

$$\frac{1}{1 + i\,\alpha_{\rm eff}\,\omega\,\widehat{K}_C(\omega)} = 1 - i\,\alpha_{\rm eff}\,\omega\,\widehat{K}_C(\omega) + \mathcal{O}(\varepsilon^2), \tag{84}$$

with $\varepsilon(\omega)$ defined in Eq. (78). Thus the response-level perturbative condition is

$$\left|\alpha_{\rm eff}\,\omega\,\widehat{K}_C(\omega)\right| \ll 1 \tag{85}$$

throughout the measurement band.

Exponential kernel

For the exponential kernel,

$$K_C(t) = \tau^{-1} e^{-t/\tau} H(t), \qquad \widehat{K}_C(\omega) = \frac{1}{1 + i\omega\tau}, \tag{86}$$

so

$$\varepsilon(\omega) = \alpha_{\rm eff}\,\omega\,\frac{1}{1 + i\omega\tau}, \tag{87}$$

and hence

$$|\varepsilon(\omega)| = |\alpha_{\rm eff}|\,\frac{\omega\tau}{\sqrt{1 + (\omega\tau)^2}}. \tag{88}$$

Defining the dimensionless scan variable

$$x \equiv \omega\tau, \tag{89}$$

this becomes

$$|\varepsilon(\omega)| = |\alpha_{\text{eff}}| \, \frac{x}{\sqrt{1+x^2}}. \tag{90}$$

Near the peak-response regime $x \sim 1$, perturbative control therefore requires

$$\alpha_{\text{eff}} \ll 1. \tag{91}$$

This is the basic reason why benchmarks such as $\alpha_{\text{eff}} = 0.10$ are not ideal for an EFT-truncation narrative: they are not tiny, and they place the deformation parameter at the $\sim 10^{-1}$ level precisely in the frequency region of greatest interest.

Additional control assumptions

In addition to Eq. (88), the following conditions underlie the phenomenological sector:

1. **Weak-field linearization:** $|h_{\mu\nu}| \ll 1$, so that linearized curvature response is valid.
2. **Controlled EFT truncation:** the retained memory operator is assumed to dominate over higher-order operators in the weak-curvature, small-coupling regime [18, 19].
3. **Kernel validity band:** the exponential kernel is interpreted as a one-timescale response model, valid over a finite frequency interval rather than as an exact universal kernel [3, 4, 6].

A.2 EFT Interpretation of α_0 and τ

As discussed in the main text, general-relativistic EFT does not uniquely determine the values of α_0 or τ. Instead, these parameters should be interpreted as phenomenological response coefficients arising from coarse-graining over higher-energy gravitational dynamics, or equivalently from integrating out a higher-energy sector of the theory. Dimensional analysis suggests that τ should correspond to the characteristic timescale of the eliminated degrees of freedom, while α_{eff} parameterizes the relative strength of the resulting nonlocal correction. In the absence of a specific microscopic model these parameters cannot be predicted *a priori* and must instead be constrained experimentally, as illustrated by the exclusion curves derived in Section 5. For laboratory modulation frequencies of order $f \sim 10\,\text{Hz}$, the peak-response condition $\omega\tau \sim 1$ corresponds to an effective response timescale $\tau \sim 10^{-2}\,\text{s}$, which serves as a representative benchmark for the phenomenological analysis. The perturbative analysis above treats (α_0, τ) as phenomenological response parameters. It is useful to briefly summarize their possible EFT interpretations.

A useful phenomenological interpretation is as follows:

1. α_0 is a Wilson-type coupling controlling the strength of the leading curvature-memory operator and must therefore be bounded experimentally rather than derived from EFT alone [19, 18].

2. τ is an effective relaxation or correlation time characterizing the eliminated sector. Depending on the underlying mechanism, it may be interpreted as:

   (a) a Compton-scale timescale $\tau \sim 1/m$ from integrating out a massive mode,

   (b) an effective bath correlation time in a Mori–Zwanzig / generalized-Langevin sense [3, 4],

   (c) or a phenomenological hereditary timescale analogous in spirit to time-nonlocal tail effects in gravitational EFT [20, 21].

Accordingly, the most defensible interpretation of the present model is as a two-parameter response theory in $(\alpha_{\text{eff}}, \tau)$, to be constrained empirically rather than fixed *a priori*.

A.3 Accuracy of the Small-α_{eff} Phase Approximation

For the exponential kernel, the exact phase lag is

$$\phi_{\text{mem}}^{\text{exact}}(x) = -\arctan\left(\frac{\alpha_{\text{eff}} x}{1 + (1+\alpha_{\text{eff}})x^2}\right), \qquad x \equiv \omega\tau, \tag{92}$$

while the leading-order small-coupling approximation is

$$\phi_{\text{mem}}^{\text{LO}}(x) \approx -\alpha_{\text{eff}} \frac{x}{1+x^2}. \tag{93}$$

Define the relative error

$$\text{Err}_{\text{rel}}(\alpha_{\text{eff}}, x) \equiv \frac{|\phi_{\text{mem}}^{\text{exact}}(x) - \phi_{\text{mem}}^{\text{LO}}(x)|}{|\phi_{\text{mem}}^{\text{exact}}(x)|}. \tag{94}$$

A representative summary over $\alpha_{\text{eff}} \in [10^{-4}, 10^{-1}]$ and $\omega\tau \in [10^{-2}, 10]$ is shown in Table 2.

Table 2: Representative error summary for the leading-order small-α_{eff} phase approximation.

α_{eff}	max abs. error (rad)	rel. error at $\omega\tau = 1$	$\phi_{\text{mem}}^{\text{exact}}(\omega\tau = 1)$ (rad)
10^{-4}	3.25×10^{-9}	5.0×10^{-5}	-5.0×10^{-5}
10^{-3}	5.77×10^{-7}	6.7×10^{-4}	-5.0×10^{-4}
10^{-2}	1.01×10^{-4}	8.9×10^{-3}	-3.7×10^{-3}
10^{-1}	3.04×10^{-3}	5.1×10^{-2}	-4.76×10^{-2}

The main conclusion is therefore:

1. For $\alpha_{\text{eff}} \leq 10^{-3}$, the leading-order approximation is extremely accurate across the full scan range.

2. For $\alpha_{\text{eff}} \sim 10^{-2}$, the approximation remains percent-level accurate near $\omega\tau \sim 1$.

3. For $\alpha_{\text{eff}} \sim 10^{-1}$, the approximation is visibly imperfect and is not ideal for a controlled small-coupling benchmark.

A conservative illustrative benchmark should therefore use

$$\alpha_{\text{eff}} \lesssim 10^{-2}, \tag{95}$$

and preferably $\alpha_{\text{eff}} \sim 10^{-3}$–$10^{-2}$.

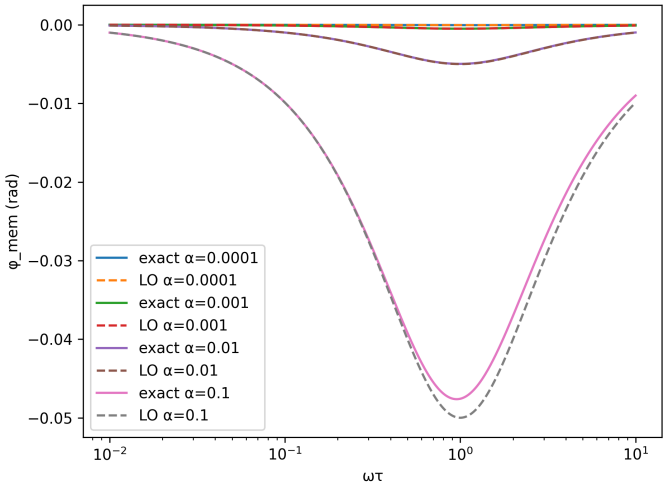

Figure 2: Exact exponential-kernel phase lag compared with the leading-order small-α_{eff} approximation across the scan range $\omega\tau \in [10^{-2}, 10]$ for representative couplings. The approximation remains highly accurate for $\alpha_{\text{eff}} \lesssim 10^{-3}$ and percent-level accurate near $\omega\tau \sim 1$ for $\alpha_{\text{eff}} \sim 10^{-2}$.

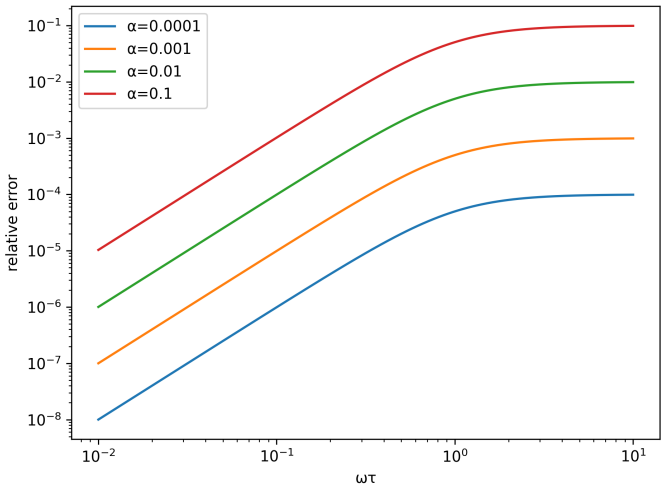

Figure 3: Relative error of the leading-order phase approximation compared to the exact exponential-kernel solution across the scan range $\omega\tau \in [10^{-2}, 10]$. The error remains below the percent level for $\alpha_{\rm eff} \lesssim 10^{-2}$ near the peak-response region $\omega\tau \sim 1$.

The agreement between the exact exponential-kernel phase lag and the leading-order approximation is illustrated in Fig. 2, while the corresponding relative error across the scan range is shown in Fig. 3.

A.4 Explicit Observable Closure: $\delta R \to \delta\Phi \to \delta a \to \Delta\Phi_{\rm AI}$

Section 5 introduced the observable mapping from the scalar-curvature response to the interferometric phase measured by an atom interferometer. In this appendix we provide the detailed derivation of that mapping, beginning from the weak-field Newtonian limit and propagating the response through the acceleration channel to the interferometric phase observable.

Fourier-space transfer from curvature to acceleration

In the weak-field, slow-motion regime, the spacetime metric may be written

$$g_{00} \simeq -(1 + 2\Phi/c^2), \tag{96}$$

so that the Newtonian potential Φ determines the inertial acceleration

$$\mathbf{a} = -\nabla\Phi. \tag{97}$$

To connect the curvature perturbation δR to the Newtonian potential, we combine the Poisson equation

$$\nabla^2\delta\Phi = 4\pi G\,\delta\rho, \tag{98}$$

with the trace-sourced curvature relation used in the matter-coupled regime of the present framework,

$$\delta R \simeq -\frac{8\pi G}{c^2}\,\delta\rho. \tag{99}$$

Eliminating $\delta\rho$ between Eqs. (98) and (99) gives

$$\nabla^2\delta\Phi = -\frac{c^2}{2}\,\delta R. \tag{100}$$

This relation follows from the trace-sourced curvature scaling used in the matter-coupled regime of the present framework (Section 5) and therefore adopts the same trace-sign convention.

Transforming Eq. (100) to spatial Fourier space ($\nabla \to i\mathbf{k}$, $\nabla^2 \to -k^2$) yields

$$\delta\Phi(\mathbf{k},\omega) = \frac{c^2}{2k^2}\,\delta R(\mathbf{k},\omega). \tag{101}$$

Taking the gradient to obtain the acceleration then gives

$$\delta\mathbf{a}(\mathbf{k},\omega) = -\frac{c^2}{2}\,\frac{i\mathbf{k}}{k^2}\,\delta R(\mathbf{k},\omega). \tag{102}$$

This relation closes the observable pipeline: the same complex memory response appearing in $\delta R(\omega)$ propagates through the Newtonian potential to the measurable acceleration perturbation $\delta a(\omega)$.

Compact source-to-observable response. Using $\delta R(\mathbf{k},\omega) = \chi_{\rm eff}(\omega)\,\delta p(\mathbf{k},\omega)$ together with the Newtonian-limit mapping to the acceleration channel, the interferometric response may be written directly as

$$\Delta\Phi_{\rm AI}(\mathbf{k},\omega) = -\,k_{\rm eff}T^2\,\frac{c^2}{2}\,\frac{i\,\mathbf{k}\cdot\hat{\mathbf{e}}}{k^2}\,\chi_{\rm eff}(\omega)\,\delta p(\mathbf{k},\omega). \tag{103}$$

Equation (103) shows that the memory-induced phase lag enters the measured signal entirely through the complex scalar susceptibility $\chi_{\rm eff}(\omega)$, which for the exponential kernel takes the form $\chi_{\rm eff}(\omega) = \chi/(1 + i\alpha_{\rm eff}\omega\widehat{K}_C(\omega))$.

Transfer-function interpretation. Equation (103) may be interpreted as the frequency-domain transfer function connecting the driven source perturbation δp to the measured interferometric phase. Defining

$$H(\mathbf{k},\omega) \equiv \frac{\Delta\Phi_{\rm AI}(\mathbf{k},\omega)}{\delta p(\mathbf{k},\omega)}, \tag{104}$$

the experiment directly measures the complex response

$$H(\mathbf{k},\omega) = -\,k_{\rm eff}T^2\frac{c^2}{2}\,\frac{i\,\mathbf{k}\cdot\hat{\mathbf{e}}}{k^2}\chi_{\rm eff}(\omega). \tag{105}$$

The phase of this transfer function therefore contains the memory-induced phase lag

$$\phi_{\rm mem}(\omega) = \arg[\chi_{\rm eff}(\omega)]\,, \tag{106}$$

which may be extracted experimentally through lock-in detection of the response quadrature at the driving frequency.

Atom interferometer phase response

For a light-pulse atom interferometer (AI), the phase response to an approximately uniform acceleration perturbation is

$$\Delta\Phi_{\rm AI} \simeq k_{\rm eff}\,\delta a\,T^2, \tag{107}$$

where $k_{\rm eff}$ is the effective wavevector and T is the pulse separation time [16].

Thus the measured signal may be written as

$$\Delta\Phi_{\rm AI}(\omega) = k_{\rm eff}T^2\,\delta a_{\rm GR}(\omega)\,\frac{1}{1+i\alpha_{\rm eff}\omega\widehat{K}_C(\omega)}. \tag{108}$$

The measured phase-lag signal is therefore exactly

$$\phi_{\rm mem}(\omega) = \arg[\chi_{\rm eff}(\omega)], \tag{109}$$

now mapped explicitly into the acceleration-sensitive channel.

Worked numerical benchmark

Consider the following controlled near-field source configuration:

$$M = 100\ \text{kg}, \tag{110}$$

$$r_0 = 0.20\ \text{m}, \tag{111}$$

$$\Delta r = 0.01\ \text{m}, \tag{112}$$

so that

$$\frac{\Delta r}{r_0} = 0.05. \tag{113}$$

Take representative atom-interferometer parameters

$$k_{\rm eff} = 1.6\times10^7\ \text{m}^{-1}, \qquad T = 0.50\ \text{s}, \tag{114}$$

and choose the drive frequency

$$f = 10\ \text{Hz}, \qquad \omega = 2\pi f, \qquad \tau = \omega^{-1} \simeq 0.0159\ \text{s}, \tag{115}$$

so that

$$\omega\tau = 1. \tag{116}$$

The benchmark $\omega\tau = 1$ corresponds to the peak-response regime of the exponential kernel and is used only as an illustrative sensitivity estimate. The

experimental analysis itself constrains the full $(\alpha_{\rm eff}, \tau)$ parameter space through the exclusion curves derived below and does not assume a priori tuning of τ to the drive frequency.

The GR acceleration modulation amplitude is then

$$\delta a_0 \simeq 2\frac{\Delta r}{r_0}\frac{GM}{r_0^2} = 2\frac{GM\,\Delta r}{r_0^3} \approx 1.67 \times 10^{-8}\ \mathrm{m\,s^{-2}}. \tag{117}$$

The corresponding GR interferometric phase amplitude is

$$|\Delta\Phi_0| \simeq k_{\rm eff} T^2\, \delta a_0 \approx 0.0667\ \mathrm{rad}. \tag{118}$$

For representative small couplings, the memory-induced phase lag at $\omega\tau = 1$ is summarized in Table 3.

Table 3: Representative benchmark values at $f = 10$ Hz and $\omega\tau = 1$.

$\alpha_{\rm eff}$	$\phi_{\rm mem}$ (rad)	$\lvert\phi_{\rm mem}\rvert/\omega$ (s)
10^{-4}	-5.0×10^{-5}	8.0×10^{-7}
10^{-3}	-5.0×10^{-4}	8.0×10^{-6}
2×10^{-3}	-9.99×10^{-4}	1.59×10^{-5}
10^{-2}	-4.98×10^{-3}	7.9×10^{-5}

The measured phase time series therefore takes the form

$$\Delta\Phi_{\rm AI}(t) \approx |\Delta\Phi_0| \cos(\omega t + \phi_{\rm mem}), \tag{119}$$

so that a lock-in measurement of the response quadrature at the drive frequency directly estimates $\phi_{\rm mem}$.

A.5 Exclusion Curves Rather Than Single-Point Constraints

In the small-coupling regime, the exponential-kernel phase lag is approximated by

$$\phi_{\rm mem}(\omega) \approx -\alpha_{\rm eff}\frac{\omega\tau}{1 + (\omega\tau)^2}. \tag{120}$$

If the response phase is measured with uncertainty σ_ϕ, then non-observation implies

$$|\phi_{\rm mem}(\omega)| \le \sigma_\phi, \tag{121}$$

which yields the exclusion curve

$$\alpha_{\rm eff,max}(\tau; \sigma_\phi, \omega) \approx \sigma_\phi \frac{1 + (\omega\tau)^2}{\omega\tau}. \tag{122}$$

For a representative sensitivity

$$\sigma_\phi = 10^{-3}\ \mathrm{rad}, \tag{123}$$

the minimum reachable coupling is

$$\alpha_{\mathrm{eff,max}}^{\mathrm{min}} = 2\sigma_\phi = 2 \times 10^{-3}, \tag{124}$$

attained at

$$\omega\tau = 1. \tag{125}$$

Thus the correct exclusion statement is two-dimensional in $(\alpha_{\mathrm{eff}}, \tau)$, not a single benchmark point. The exclusion curves shown in Fig. 4 illustrate the accessible region of the $(\alpha_{\mathrm{eff}}, \tau)$ parameter space.

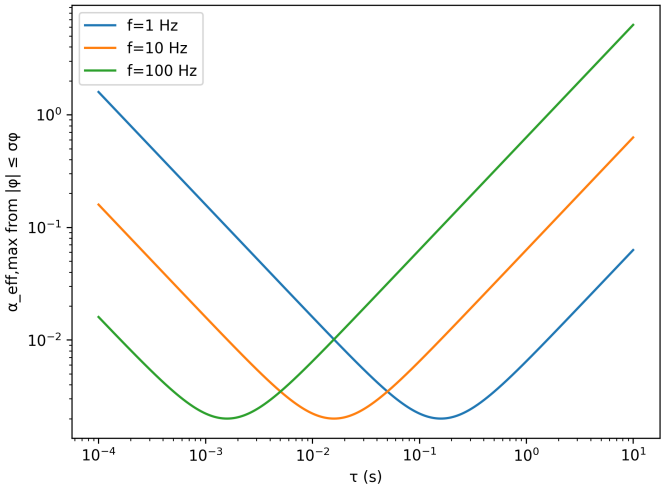

Figure 4: Representative exclusion curves for the curvature-memory coupling α_{eff} as a function of the memory timescale τ for an interferometric phase sensitivity $\sigma_\phi = 10^{-3}$ rad. The minimum reachable coupling occurs near $\omega\tau = 1$, where $\alpha_{\mathrm{eff}}^{\mathrm{min}} \approx 2\sigma_\phi$.

Relation to existing experimental constraints. Existing laboratory measurements of gravitational acceleration, including atom-interferometric experiments and precision gravimetry (e.g. [16, 24]), primarily constrain static or quasi-static deviations from Newtonian gravity. In the curvature–memory framework developed here, the predicted observable signature is not a static acceleration offset but a frequency-dependent phase lag in the driven response.

In the static limit $\omega \to 0$, the memory response reduces continuously to the general-relativistic result, so existing static measurements primarily constrain only this low-frequency limit. Consequently, current datasets do not yet provide strong bounds on the parameter region near the peak-response condition $\omega\tau \sim 1$ explored in the benchmark analysis. Dedicated modulated-source experiments or interferometric phase-lag measurements would therefore be required to probe this regime directly.

A.6 Assumptions and Caveats

The foregoing analysis rests on the following assumptions:

1. **Linear response:** the driven source remains within the scalar linear-response regime.
2. **Weak-field / slow-motion limit:** the mapping from δR to $\delta\Phi$ and δa uses the Newtonian/quasi-static limit.
3. **Near-field apparatus geometry:** the device is sufficiently close to the driven source that the dominant response is sourced by matter-coupled curvature rather than vacuum wave propagation.
4. **Kernel-model dependence:** the exponential kernel is a one-timescale ansatz and does not claim to represent the unique admissible response kernel.
5. **EFT truncation:** the retained memory term is treated as the leading operator in the relevant weak-curvature, small-coupling sector.

Within these assumptions, the framework supports the following conclusions:

1. there is a controlled perturbative regime $|\varepsilon(\omega)| \ll 1$ in which the memory sector is a small deformation of GR response;
2. the parameters (α_0, τ) are best interpreted as phenomenological response parameters to be bounded experimentally;
3. the observable pipeline closes explicitly through the chain $\delta R \to \delta\Phi \to \delta a \to \Delta\Phi_{\mathrm{AI}}$;
4. a controlled benchmark with $\Delta r/r_0 \leq 0.05$ yields a measurable phase amplitude and a direct phase-lag observable;
5. the proper falsifiability statement is an exclusion curve in the $(\alpha_{\mathrm{eff}}, \tau)$ plane.

Funding

This research received no external funding.

Competing Interests

The author declares no competing interests.

Data Availability

No datasets were generated or analyzed during the current study.

Declaration of Generative AI and AI-Assisted Technologies

During the preparation of this manuscript, the author used an AI-assisted language model (ChatGPT, OpenAI) for limited editorial assistance, including language clarification and structural organization. All scientific content, mathematical derivations, analysis, and conclusions were developed, reviewed, and verified by the author, who takes full responsibility for the work.

References

[1] Einstein, A.: The foundation of the general theory of relativity. *Ann. Phys.* **49**, 769–822 (1916)

[2] Donoghue, J.F.: Quantum gravity as a low-energy effective field theory. *Scholarpedia* **12**(4), 32997 (2017)

[3] Kubo, R.: The fluctuation–dissipation theorem. *Rep. Prog. Phys.* **29**, 255–284 (1966)

[4] Zwanzig, R.: Nonlinear generalized Langevin equations. *J. Stat. Phys.* **9**, 215–220 (1973)

[5] Bagley, R.L., Torvik, P.J.: A theoretical basis for the application of fractional calculus to viscoelasticity. *J. Rheol.* **27**, 201–210 (1983)

[6] Mainardi, F.: Fractional relaxation–oscillation and fractional viscoelasticity. *Chaos Solitons Fractals* **7**, 1461–1477 (1996)

[7] Hu, B.L.: Stochastic gravity. *Int. J. Theor. Phys.* **38**, 2987–3037 (1999)

[8] Martín, R., Verdaguer, E.: Stochastic semiclassical gravity. *Phys. Lett. B* **465**, 113–117 (1999)

[9] Hu, B.L., Verdaguer, E.: Stochastic gravity: Theory and applications. *Living Rev. Relativ.* **11**, 3 (2008)

[10] Maggiore, M.: Nonlocal infrared modifications of gravity: a review. *Fundam. Theor. Phys.* **187**, 221–281 (2017)

[11] Sotiriou, T. P., Faraoni, V.: f(R) theories of gravity. *Rev. Mod. Phys.* **82**, 451–497 (2010)

[12] De Felice, A., Tsujikawa, S.: f(R) theories. *Living Rev. Relativ.* **13**, 3 (2010)

[13] Brans, C., Dicke, R. H.: Mach's principle and a relativistic theory of gravitation. *Phys. Rev.* **124**, 925 (1961)

[14] Clifton, T., Ferreira, P. G., Padilla, A., Skordis, C.: Modified gravity and cosmology. *Phys. Rep.* **513**, 1–189 (2012)

[15] E. Noether, Invariante Variationsprobleme, *Nachr. D. König. Gesellsch. D. Wiss. Göttingen, Math.-Phys. Kl.* **1918**, 235 (1918).

[16] Cronin, A.D., Schmiedmayer, J., Pritchard, D.E.: Optics and interferometry with atoms and molecules. *Rev. Mod. Phys.* **81**, 1051–1129 (2009)

[17] Asenbaum, P., Overstreet, C., Kim, M., Curti, J., Kasevich, M.A.: Atom-interferometric test of the equivalence principle at the 10^{-12} level. *Phys. Rev. Lett.* **125**, 191101 (2020)

[18] Donoghue, J.F.: General relativity as an effective field theory: The leading quantum corrections. *Phys. Rev. D* **50**, 3874–3888 (1994)

[19] Burgess, C.P.: Quantum gravity in everyday life: General relativity as an effective field theory. *Living Rev. Relativity* **7**, 5 (2004)

[20] Poisson, E., Pound, A., Vega, I.: The motion of point particles in curved spacetime. *Living Rev. Relativity* **14**, 7 (2011)

[21] Galley, C.R.: Classical mechanics of nonconservative systems. *Phys. Rev. Lett.* **110**, 174301 (2013)

[22] Adelberger, E.G., Heckel, B.R., Nelson, A.E.: Tests of the gravitational inverse-square law. *Ann. Rev. Nucl. Part. Sci.* **53**, 77–121 (2003)

[23] Kapner, D.J., Cook, T.S., Adelberger, E.G., Gundlach, J.H., Heckel, B.R., Hoyle, C.D., Swanson, H.E.: Tests of the gravitational inverse-square law below the dark-energy length scale. *Phys. Rev. Lett.* **98**, 021101 (2007)

[24] Peters, A., Chung, K.Y., Chu, S.: Measurement of gravitational acceleration by dropping atoms. *Nature* **400**, 849–852 (1999)

[25] Asenbaum, P., Overstreet, C., Kim, M., Curti, J., Kasevich, M.A.: Phase shift in an atom interferometer due to spacetime curvature. *Phys. Rev. Lett.* **118**, 183602 (2017)